Published in final edited form as:

Neurobiol Aging. 2017 August ; 56: 87–99. doi:10.1016/j.neurobiolaging.2017.04.003.

Increasing GABA reverses age-related alterations in excitatory receptive fields and intensity coding of auditory midbrain neurons in aged mice

Elliott J. Brecht[a,b], **Kathy Barsz**[c], **Benjamin Gross**[b,d], and **Joseph P. Walton**[a,b,e,*]

[a]Department of Chemical and Biomedical Engineering, University of South Florida, Tampa, FL, USA

[b]Global Center of Speech and Hearing Research, University of South Florida, Tampa, FL, USA

[c]School of Nursing, University of Rochester, Rochester, NY, USA

[d]Department of Physics, University of South Florida, Tampa, FL, USA

[e]Department of Communication Sciences and Disorders, University of South Florida, Tampa, FL, USA

Abstract

A key feature of age-related hearing loss is a reduction in the expression of inhibitory neurotransmitters in the central auditory system. This loss is partially responsible for changes in central auditory processing, as inhibitory receptive fields play a critical role in shaping neural responses to sound stimuli. Vigabatrin (VGB), an antiepileptic agent that irreversibly inhibits γ-amino butyric acid (GABA) transaminase, leads to increased availability of GABA throughout the brain. This study used multi-channel electrophysiology measurements to assess the excitatory frequency response areas in old CBA mice to which VGB had been administered. We found a significant post-VGB reduction in the proportion of V-type shapes, and an increase in primary-like excitatory frequency response areas. There was also a significant increase in the mean maximum driven spike rates across the tonotopic frequency range of all treated animals, consistent with observations that GABA buildup within the central auditory system increases spike counts of neural receptive fields. This increased spiking is also seen in the rate-level functions and seems to explain the improved low-frequency thresholds.

Keywords

Midbrain; Electrophysiological recording; Inferior colliculus; Presbycusis; eFRA; Inhibition; GABA; Vigabatrin

*Corresponding author at: Department of Communication Sciences and Disorders, University of South Florida, 4202 Fowler Av, Tampa, FL 33647, USA. Tel.: (813) 974-4080; fax: (813) 905-9840. jwalton1@usf.edu (J.P. Walton).

Disclosure statement

The authors have no actual or potential conflicts of interest.

1. Introduction

There are at least 2 underlying etiologies that accompany age-related hearing loss (ARHL), impaired peripheral sensitivity and deficits in central auditory processing. While peripheral hearing loss can alter a listener's speech recognition abilities, increasing evidence indicates that aged animals and humans with normal peripheral hearing can show impaired auditory perception (Barsz et al., 2002; Frisina and Frisina, 1997; Grose and Mamo, 2010; Walton et al., 2008). There is also strong evidence that changes in neurotransmitter levels are at least partly responsible for these age-related changes in central auditory processing and underlie many of the physiological changes seen in neural responses from the central auditory system (Arivazhagan and Panneerselvam, 2002; Caspary et al., 1995; Gleich and Strutz, 2011; Helfert et al., 2002, 2003; Shaddock Palombi et al., 2001; Turner et al., 2013). In the auditory midbrain, inhibitory receptive fields are formed primarily by γ-aminobutyric acid $(GABA)_A$ receptors, which are mediated by the convergence of the neuronal projections from nuclei in the auditory brainstem (Palombi and Caspary, 1996). These projections play a critical role in shaping the robust and specific neuronal responses to sound stimuli by sharpening the neural filters, consequently removing noise from the processed signal (Caspary et al., 2002; Mossop et al., 2000; Rees and Moller, 1983, 1987). A number of studies have shown that the reductions in inhibitory neurotransmitter expression and changes in central auditory system processing associated with aging may contribute to the diminished ability to process complex sound stimuli (Caspary et al., 1995, 2008; Helfert et al., 2003; Leong et al., 2011; Turner et al., 2005a; Willott et al.,1991).

Vigabatrin (VGB) is typically used as an antiepileptic agent (Ben-Menachem and Sander, 2011) and irreversibly inhibits GABA transaminase by preventing its catabolism through selective interactions with the enzymes that metabolize GABA (Ben-Menachem and Sander, 2011; Brozoski et al., 2007; Caspary et al., 1995; Faingold et al., 1989, 1991; Gleich et al., 2003; Gram et al., 1989). Without this catabolic recycling, excess GABA naturally accumulates in the postsynaptic space, which is why treatment with VGB increases the concentration levels of GABA throughout nerve terminals, rendering more available for synaptic transmission (Mattson et al., 1995). Functional changes in GABAergic circuitry in the auditory cortex (AC) have also been shown with aging, though the specific mechanisms that link the 2 are still unknown (Llano et al., 2012; Turner et al., 2013). These findings of GABAergic changes are congruent with multiple studies which have found that the age-dependent decline in auditory temporal processing cannot be attributed solely to peripheral hearing loss (Barsz et al., 2002; Grose and Mamo, 2010; Ohlemiller and Frisina, 2008; Parthasarathy and Bartlett, 2011; Walton et al., 2008). The present study was in part motivated by a report from Gleich and et al. which demonstrated that aged gerbils with deficits in behavioral gap detection (i.e., higher gap detection thresholds) showed significant improvements in minimal gap thresholds following treatment with VGB (Gleich and Strutz, 2011; Gleich et al., 2003). The VGB-induced improvement was greatest in groups with impaired temporal processing (typically older animals), whereas in animals that exhibited good temporal resolution before treatment no effect of treatment was found. Overall, they found that treatment with VGB improved the behavioral gap detection thresholds of older

gerbils, so that they were similar to those of the young controls (Gleich and Strutz, 2011; Gleich et al., 2003).

The inferior colliculus (IC) is the main auditory relay center located within the midbrain, and receives complex afferent input from both contralateral and ipsilateral nuclei. As a result, virtually all acoustic information passes through the IC, making it a key nucleus for all ascending information (Aitkin, 1986; Frisina and Walton, 2001b). Projections from lower nuclei terminate at specific locations along the isofrequency laminae of the IC and form complex parallel processing networks (Stiebler and Ehret, 1985; Willott et al., 1985, 1991). The interplay of excitation and inhibition is one mechanism which modulates these neural networks with the main inhibitory neurotransmitter being GABA (Faingold, 2002; Faingold et al., 2000). GABA agonist and antagonist have been shown to alter both spectral and temporal neural processing in the IC (Covey and Casseday, 1999; Faingold, 2002; Herrmann et al., 2015; Parthasarathy et al., 2010; Pedemonte et al., 1997).

The majority of auditory midbrain excitatory frequency response areas (eFRAs) are V-shaped, and a lower number of these are seen in the responses of aged mice in comparison to young and middle-aged animals (Leong et al., 2011). Similarly, eFRAs within the AC exhibit age-related changes comparable to those seen in the IC. Turner et al. found a decrease in the occurrence of V- and U-shaped eFRAs (Turner et al., 2005a,b). This is concurrent with an increase in the number of complex eFRAs in aged rats. They also reported an increase in discharge rate in response to extracellular current pulses, though eFRAs for aged animals were less consistent across multiple repetitions (Turner et al., 2005a,b). However, there was a reduction in the presence of inhibitory side bands for responses from IC neurons in older mice (Brimijoin and Walton, 2008). This occurred with post-excitatory suppression being closely tied to the excitation strength and an overall reduction in frequency specificity (Brimijoin and Walton, 2008). There is still a debate over whether there is a clearly defined set of eFRA types, or if some neurons exhibit responses that are intermediate classifications or contain characteristics of several of these based on their inhibitory and excitatory projections (Palmer et al., 2013). For this study, we settled on a set of classification types similar to those described in a study by Willott et al., without categorizing every possible continuum (Willott et al., 1984).

Previous reports have shown that systemic administration of VGB can reduce tinnitus and improve temporal processing, identified using behavioral measures in rodents (Brozoski et al., 2007; Gleich and Strutz, 2011; Gleich et al., 2003, 2014). This suggests that alterations in GABAergic neurotransmission have therapeutic potential. Our goal was to test the hypothesis that systemic treatment with VGB in old CBA mice would sharpen the receptive fields of auditory midbrain neurons. Such a finding would suggest that modulation of GABAergic effects in the IC leads to changes in frequency-specific processing, in addition to the known suppression of tinnitus and improvement of gap detection. This would mean that modulation of GABAergic circuitry could potentially improve spectral resolution as well as other complex listening tasks, such as speech in noise perception.

2. Materials and methods

2.1. Subjects

Multi-channel recordings were taken from 38 old (>24 months) mixed gender CBA/CaJ mice (15 VGB and 23 control). CBA/CaJ mice were chosen because the loss of peripheral function is similar to humans, making them a good model for the study for ARHL (Frisina and Walton, 2001a,b; Ohlemiller and Frisina, 2008; Ohlemiller et al., 2010). The CBA/CaJ mouse strain is commonly used in animal models of ARHL, and several studies have shown that this strain of laboratory mouse shows relatively little age-related hearing loss and hair cell loss until very late in their life span (Henry and Chole, 1980; Li and Borg, 1991; Spongr et al., 1997). This strain loses hearing sensitivity very slowly, at a rate comparable to the slowest progression rates of human ARHL, normalizing for lifespan (Ohlemiller and Frisina, 2008). Moreover, for the most part the hearing loss is relatively flat or slightly greater for the high frequencies, equivalent to “golden ears” in human age-related hearing loss (Allen and Eddins, 2010). Founder breeding pairs were obtained from The Jackson Laboratory (Bar Harbor, ME, USA) and were bred within the facilities of the university vivarium and housed 3–4 per cage with litter-mates in rodent micro-isolator cages (36.9 ×15.6 × 13.2 cm) kept near 25 °C, on a 12/12 hours light/dark cycle with ad lib water and food pellets. Cages were changed weekly, and the mice were monitored for signs of distress several times throughout the day. Only nulliparous mice were used for experiments. All procedures were preapproved by the University of Rochester Committee on Animal Resources and are consistent with US Federal and NIH guidelines under IACUC protocol #220-D.

2.2. Surgical preparation

The mice were initially anesthetized with an intraperitoneal (i.p.) injection of ketamine and xylazine (100 mg/kg and 10 mg/kg). After the anesthesia was induced, the top of the animal’s head and neck was then shaved of fur to prevent contamination of the incision site. The skin was cleaned with germicidal scrub, rinsed with 70% alcohol, and prepped with iodine. The skull was then exposed, 2% lidocaine was applied to the site of incision, and a small brass tube was secured to the skull surface along the sagittal suture at bregma with vet bond and adhered with dental cement. Mice were given a recovery period of 24–48 hours before beginning the experimental sessions.

2.3. Drug administration

VGB was prepared from commercially available sachets (Aventis Pharma Kent, UK, 500 mg pure VGB powder) and administered to old CBA mice (n = 15) via an i.p. injection at a dose of 50 mg/kg, a dosage similar to several studies implicated by Gleich et al. (2014). Fresh solutions were made before each experiment. In the age-matched control mice (n = 23), a saline injection was administered. Previous studies in mice have shown that peak serum levels of VGB are reached within 1–2 hours following i.p. injection (Johannessen and Tomson, 2006; Rey et al., 1992).

2.4. Recording procedures

The right IC was stereotaxically located (Paxinos and Franklin, 2001) and exposed via a small (<1.0 mm) craniotomy. Before recording, chlorprothixene (Taractin, 5–12 mL/g i.m.) was administered to prevent involuntary movement via inhibition of para-sympathetic nerve impulses. The animal was then secured in a custom stereotaxic frame (Newport-Klinger) in a heated (34 °C) chamber lined with sound-absorbing foam (Sonex). Multi-unit extracellular activity was recorded using vertically oriented single shank silicon acute penetrating 16-channel electrodes with an impedance ranging from 1.2 to 2.1 MΩ (Type-A, 3 mm ×100 μm; NeuroNexus Technologies). The electrode was positioned stereotaxically over the IC after reference to the lambda landmark on the skull and was advanced dorsoventrally into the IC by a micro positioner (Newport-Klinger PMC 100). The output from the electrode was attached to a low noise (5–6 μV noise floor) preamplifier (RA16), having an operating range of ±7 mV. Neural events were acquired and visualized in real-time using the OpenEx software platform (TDT, Inc) and a custom designed MATLAB (The MathWorks, Inc, Matick, MA, USA) graphical interface. Neural recordings from each channel were then filtered (300–3000 Hz), amplified, and sampled at 25 kHz in a 1.25-ms time window subsequent to the event crossing a voltage discriminator. A spike triggering threshold of 4:1 signal-to-noise ratio was automatically set for all channels. The search signal used to estimate the spike triggering thresholds was a 50-ms broadband noise stimulus presented at 60 dB SPL at a rate of 5/s. Each penetration typically yielded 8–12 active channels. Recording sessions lasted an average of 6–8 hours, and if at any time a mouse showed signs of discomfort, like excessive movement, it was removed from the apparatus and testing was halted.

2.5. Stimulus generation and presentation

Noise and tone bursts were generated digitally (Real-time Processor Visual Design Studio, TDT) using a System 3 processor and D/A converter (TDT RX6) with 200 kHz sampling rate. The signals were routed to an electrostatic speaker (TDT ES1) with a flat frequency response from 4 to 110 kHz. This speaker was placed at 60° azimuth contralateral to the recording site. Harmonic distortions were measured with a Dynamic Signal Analyzer (HP 35665A) and were at least 60 dB below the primary signal. The distance between the speaker and the pinna was fixed at 22.5 cm and calibrated using a B&K 2610 amplifier and a ¼″ microphone placed at the location of the pinna. eFRAs from all active channels were acquired simultaneously using 25 ms (5 ms rise/fall) tone burst stimuli presented from 0 to 80 dB SPL in 5 dB steps and from 2 to 64 kHz for a total of 2125 frequency and intensity combinations that were presented pseudo-randomly 5 times at a rate of 10/s.

2.6. Spike sorting

Spike waveforms were processed in MATLAB using the TDT OpenDeveloper ActiveX controls and passed to AutoClass C v3.3.4, an unsupervised Bayesian classification system that seeks a maximum posterior probability classification, developed at the NASA Ames Research Center (Cheeseman and Stutz, 1996; Stutz and Cheeseman, 1996). AutoClass scans the data set of voltage-time waveforms according to custom specified spike parameters to produce the best fit classifications of the data, which may include distinct single- and

multi-unit events, as well as noise. To discriminate the signal from noise in the present study, the variance of the background noise was estimated as the quartile range of the first 5 digitization points of the spike waveform, at these are recorded before the threshold-crossing event. To avoid overloading AutoClass with excessive noise, which leads to over-classification, this noise measure is used to screen the event waveform data, such that only voltage points with absolute values greater than this noise floor were presented for use in the classification. Once the classes had been determined in each channel of data, they were visualized within a custom MATLAB program and assigned to multi-unit, single-unit, or noise classes. Event classes which were categorized as noise were subsequently discarded, and units with distinct biphasic waveforms and good signal-to-noise ratio were classified as single units. As most channels recorded information elicited from the spiking of 2 or more neurons, all recordings units in this paper were considered to be multi-unit activity (Kirby and Middlebrooks, 2012). Nonetheless, there was no observation of any consistent differences in the eFRAs between single units and multi-unit clusters.

2.7. Data analyses

eFRAs were analyzed using a custom MATLAB program. We classified eFRA tuning using a method similar to that used to classify neurons in the primary AC (Sutter, 2000). The eFRAs were sorted into V-shaped, multi-peak, primary-like, and closed/complex by judges blind to the groups. V-shaped eFRAs become broader at higher intensities, multi-peak eFRAs have more than one distinct excitatory region separated by frequencies with little or no excitation, primary-like eFRAs have a low-frequency tail that is shallower than the high-frequency tail, and closed-complex eFRAs have an enclosed excitatory area or multiple excitatory areas that do not fit into the patterns of the first 3 types. The frequency at which driven activity is responsive at the lowest intensity (threshold) is classified as the characteristic frequency (CF) and the point in the receptive field which elicits the maximal driven activity is categorized as the best frequency (BF). A custom MATLAB program was used to calculate the edges of each channel's eFRA, and this was verified via visual inspection to ensure no nondriven activity was included in the calculation. The edges of the eFRA were defined as the activity levels that were equal to or greater than the background rate and at least 15% of the maximum rate. Each eFRA was categorized into low-BF (<15 kHz), mid-BF (15–30 kHz), and high-BF (>30 kHz) groups based on the topographical representation proposed by Willott (Willott et al., 1984). These frequency cutoffs divide the mouse IC topographic map into 3 equal dorso-ventral sections (Stiebler, 1986; Stiebler and Ehret, 1985). The bandwidth was measured based on the quality factor (Q), a measure of frequency tuning sharpness (Hernandez et al., 2005). Q10 through Q40 values were calculated using the following formula:

$$Q_{xdB} = \frac{CF}{high\ frequency\ cutoff\ -\ low\ frequency\ cutoff}$$

Q values could not be calculated for eFRAs classified as the closed-complex type, or if the high-frequency edge boundary extended above 64 kHz at 40 dB above threshold. Q40 was also not calculated if the threshold was above 40 dB SPL. The steepness of the eFRA low-

frequency and high-frequency slopes were calculated as the number of octaves between the cutoff frequencies at 10 and 40 dB above threshold.

The asymmetry index (AI) of eFRAs was calculated at 40 dB above threshold in which the distance from the high frequency (HF) edge to the CF was subtracted from the distance between the low frequency (LF) edge and the CF and then this was divided by the total bandwidth between edges (Yan et al., 2005):

$$asymmetry\ index = \frac{(CF - LF) - (HF - CF)}{(HF - LF)}$$

The calculated AI varies between ±1.0, with negative values indicating a tilt in the eFRA toward the HF side and positive numbers indicating a tilt toward the LF side. Values which are approximately 0 indicate eFRA symmetry with reference to the CF (Leong et al., 2011).

The change in the driven response due to treatment was further examined when collecting tone-induced rate-level functions (RLFs) derived from each eFRA at the CF. This was done by calculating the total number of events in response to a 25-ms CF tone presented from 0 to 80 dB SPL, in 5 dB steps, and examining the summed spikes per presentation at each intensity. From each of these eFRA presentations a tone RLF was calculated at the unit's CF from 0 to 80 dB SPL. Several parameters were derived from each unit's RLF, including the maximum rate, the driven rate at 10%, 50%, and 90% of the maximum rate, and the corresponding intensity level of the stimuli which elicited those rates. Coefficients were measured as an index of tone monotonicity and were calculated by dividing the count at the highest intensity by the maximum count. Values <0.80 indicated nonmonotonic RLFs (Barsz et al., 2007). Finally, first spike latencies were calculated as the time in which the first spike (Engineer et al., 2004) was recorded following the onset of a 70 dB broadband noise burst.

Statistical analysis and graphs were generated using GraphPad Prism version 6.01 for Windows (GraphPad Software, La Jolla, CA, USA). The majority of the results are presented using box plots which allows for mean, median, and the distribution of the data to be denoted. A 1-way ANOVA test and Tukey's repeated measures analysis procedure were used to evaluate the effects of VGB on the eFRA properties of MT, mean driven rates, and Q values. A 2-way ANOVA and Bonferroni's repeated measures test were used to evaluate divergent effects of VGB on the RLFs at increasing decibel levels, whereas a χ^2 test was performed to evaluate whether the frequencies of the eFRA types differed from the proportion of frequencies that would be expected by chance. Alpha was set at 0.05 for all statistical tests.

3. Results

eFRAs were recorded from 986 multi-unit responses (VGB = 494, control = 492) from a total of 38 mice. The eFRAs from each group were divided into 3 CF ranges: low (<15 kHz), mid (15–30 kHz), and high (>30 kHz) based on the topographical analysis of Willott (Willott et al., 1984) which divided the IC into 3 equal tonotopic ranges. Table 1 shows that CFs obtained from eFRAs recorded from VGB-treated mice were evenly distributed among low-, middle- and high-frequency ranges, whereas units from nontreated mice showed a

significantly greater number of high-CF units (+9.7%) and fewer low-CF units (−9.6%) compared with treated animals [χ^2 (2, N = 13.73) $p = 0.0010$]. The percentile of mid-CF units remained unchanged between the control and treatment groups (<0.1%). The overall distribution of individual unit BFs versus minimum threshold (MT) is shown in Fig. 1. In VGB-treated mice, mean neuronal thresholds tended to be lower (discussed in detail below) and ranged from 5 to 79 dB, as compared with units from nontreated mice. The range of CFs was similar and varied from 4 to 64 kHz, for treated as compared with 4–72 kHz for nontreated. This similarity in the CFs indicates that the sampling across the tonotopic axis of the IC in both treated and control mice was comparable.

3.1. Changes in eFRA type due to treatment

There were significant variations in the eFRA classification types between control and treatment groups. For each recorded unit, a full eFRA was collected and further classified according to its characteristic shape. Fig. 2 shows eFRAs which are representative of the 5 different types observed within all IC penetrations with the boundaries of the excitatory region marked by the solid white line. Fig. 2A shows a V-shaped unit which has similar slopes on both the low- and high-frequency (LF, HF) sides of the eFRA. This was the most prevalent type of eFRA encountered in both VGB-treated mice and control mice and accounted for 72.7% of control units. A significant reduction in the percentage of V-shaped eFRAs was seen in VGB-treated mice, where they accounted for 52.5% of the eFRAs [χ^2 (2, N = 13.65) $p = 0.0011$]. The second most frequent eFRA was U-shaped (Fig. 2C), accounting for 15.6% and 23.9% for the control and treated units, respectively. These were followed in frequency by primary-like eFRAs (Fig. 2B), which are characterized by shallow sloping LF edge and steep HF edge. These response areas accounted for 5.2% of the total control unit samples, with a significant increase to 16.9% for the treated units. The multi-peak type eFRAs have multiple excitatory areas that are separated by a nonresponsive area, as shown in Fig. 2D. These were similar in occurrence to the primary-like type, at 4.5% for control units, and only slightly reduced in the treated units at 2.8%. The final type, the closed/complex group, accounted for 1.9% of the control samples and had a slightly elevated occurrence of 3.8% in treated units. This group includes aspects from more than one of the above types and often contains an enclosed excitatory area. The overall distribution of eFRAs for both control and treated units are shown in Fig. 3 and described in Table 1. Results indicated an overall treatment effect in VGB-treated mice [χ^2 (2, N = 13.65), $p = 0.0011$] with post hoc testing indicating that there was a significant increase in U-shaped and primary-like type eFRAs and a substantial decrease in the proportion of V-shaped eFRA.

3.2. VGB alters minimum threshold

The effect of VGB on MT was dependent on the tonotopic region (CF frequency), as shown in Fig. 4. A significant main effect of treatment is evident from the differences in minimum thresholds between VGB treated and control units [$F(5, 980) = 5.789$, $p < 0.0001$], with VGB units exhibiting an average lower MT. However, this significant interaction was not the same across the tonotopic axis. For control mice, the mean threshold for low-CF units was 41 dB, as compared with units from VGB-treated mice which had a significantly lower threshold of 33 dB ($p = 0.002$), an 8 dB improvement. In high-frequency units, treatment resulted in significantly higher mean MTs increasing from 34 dB in control animals to 39 dB

in treated animals (p 0.05). Mid-CF control units showed no significant changes, with mean thresholds of 37 and 35 dB for control and treated mice, respectively.

3.3. Shifts in rate-level functions due to treatment

Tone-evoked RLFs derived from the eFRAs were used to examine treatment-related changes in tone intensity coding within the IC. To investigate these alterations, the 10%, 50%, and 90% points of the maximum rate on the RLF were calculated, these are shown in Fig. 5. The treatment had a recognizable impact on these quantities [F (23, 2894) = 86.12, $p < 0.0001$], with post hoc testing indicating significant differences in intensity coding for units acquired from treated old mice. The 50% maximum rate point was significantly increased from 1.6 to 2.6 spikes/stimulus following VGB treatment. There were also significant differences for the 90% point of maximum rate, with units from treated mice showing increased rates post-VGB from 2.9 to 4.6 spikes/stimulus. The change in rate for both the 50% and 90% points were similar to the significant differences in the overall maximum rate, where treatment increased the rate from 3 to 5 spikes/stimulus.

The shift in the RLFs following VGB administration is shown in Fig. 6. The results are again divided into low-, mid-, and high-CF groups, illustrating the intensity levels at which driven responses became significantly different. There was a significant divergence above 25 dB for frequencies <15 kHz [F (1, 285) = 40.80, ($p < 0.0001$)], above 30 dB for mid-CF units [F (1, 309) = 28.21, ($p < 0.0001$)], and above 50 dB for frequencies greater than 30 kHz [F (1, 387) = 5.815, ($p = 0.0001$)].

3.4. VGB decreases the first spike latency

FSL is known to vary both across the tonotopic axis of the IC and with age, and has also being linked to possible changes in GABAergic circuitry (Casseday et al., 2000; Walton et al., 1998). To determine if VGB altered FSL, we compared mean FSL differences between units from mice treated with VGB to control mice to 70 dB SPL noise bursts. Fig. 7 shows that mean FSL was significantly decreased from 14.4 ms (SEM = 0.2) in control units to 10.4 ms (SEM = 0.4) in units from VGB-treated animals [t(1310) = 9.6, $p < 0.0001$].

3.5. VGB and eFRA sharpness

Due to their prevalence, treatment-related changes within the V-shaped eFRA classification were examined further by dividing the 987 different control and treated units by the sharpness of their eFRAs based on their Q values. The Q values calculated at 10, 20, 30, 40, and 50 dB above MT are shown in Fig. 8. Note that Q40 and Q50 were not calculated when a unit threshold exceeded 40 dB SPL, which occurred in 321 (32.5%) of all recorded units. Using the Q40 percentile ranks as the base measurement for each CF, a Q of 2.0 (Leong et al., 2011) was identified as a breakpoint for distinguishing eFRA sharpness, as it divides the responses of the different CF categorizes above the median value. In control mice, 67.5% of the V-shaped eFRAs had broadly defined eFRAs based on the Q = 2.0 criteria, this was not significantly different from the 64.7% of broad eFRAs found in the treated mice. Q values were also analyzed to determine if there was an effect of VGB within restricted tonotopic regions. The low-CF units tended to have Q values greater than 2.0 following VGB treatment, and there was a significant increase in the percent of sharp classified units, 21%

for Q30 values [F (5, 1777) = 12.13, $p = 0.0188$]. All of the high-CF units, both control and treatment, tended toward a broader subtype shape, and VGB treatment resulted in a decrease of 13% for the Q50 values [F (5, 970) = 3.139, $p = 0.0236$]. Mid-CF units showed no statistical differences between treatment and control groups.

3.6. Changes in symmetry following VGB treatment

The symmetry of the eFRAs was quantified at 40 dB above threshold and divided into the frequency regions described earlier, shown in Fig. 9. Units from untreated mice displayed comparable mean symmetry data to previously reported results (Leong et al., 2011). Overall, the treatment had a significant effect on symmetry [F (5, 597) = 4.893, $p < 0.001$]. There were no significant changes following VGB treatment for the low-CF units, though there was a significant decrease in the tilt toward the HF side for the mid-range frequencies and a similar significant increase in the expansion of the LF edge for high-frequency units, resulting in an increase in overall symmetry. For the low-frequency regions, the control and treated units had mean AI values of −0.095 and −0.090, respectively, indicating that both had a minor tilt toward the HF edge of the eFRA region, with the treated units having less deviation from asymmetry. For mid-frequency units, there was a low-frequency tilt toward the LF edge. However, VGB treatment induced a significant decrease ($p = 0.0254$) in this tilt, trending toward complete symmetry with mean LF edge leaning toward values of 0.15 for controls and a more central and symmetric 0.05 value for treated units. Additional significant differences ($p = 0.0116$) were seen for high-frequency units, with mean values of 0.3 in the control group, indicating a tilt toward the low frequencies, and an increase in the HF edge of the treatment group to 0.19, indicating increased symmetry.

3.7. VGB alters spontaneous rate in a frequency-dependent manner

Spontaneous activity from control animals was significantly higher than those from mice treated with VGB. The data were further differentiated along the same CF groups described previously. Overall, significant treatment-induced reductions in spontaneous rate differences were found [F (5, 779) = 7.625 ($p = 0.0001$)]. However, the VGB-induced decreases in spontaneous activity (0.54–0.2 spikes/25 ms) from the low-CF units, shown in Fig. 10A, were not significant in post hoc analysis when compared with untreated units. Post hoc comparisons showed that spontaneous activity in treated mid-CF units (0.095 spikes/25 ms) were significantly lower than control units (0.83 spikes/25 ms). Post hoc comparisons also showed significant decreases in the high-CF group, with the control mean rate averaging 0.99spikes/25 ms and decreasing to 0.1 spikes/25 ms following treatment. No significant differences were seen between the different frequency regions within treated or untreated mice.

3.8. VGB increases the maximum driven activity rate

VGB treatment significantly increased the maximum driven rate to tonal stimulation in old animals across all 3 frequency groups [F (5, 980) = 32.88, ($p = 0.0001$)]. The maximum rate was taken from the best frequency of each eFRA and divided into CF groups. As shown in Fig. 10B, for low-CF units, the mean response for the control group was 4 spikes/25 ms as compared with 6.3 spikes/25 ms in units from age-matched VGB-treated animals ($p < 0.0001$). There was also a significant increase in driven activity following treatment of the

mid-CF rate, from 4.1 to 5.9 spikes/25 ms ($p < 0.001$) and high-CF rate, from 3.5 to 5.1 spikes/25 ms ($p < 0.001$).

4. Discussion

Systemic administration of VGB in our mouse model of ARHL resulted in 4 main findings. The first is that the minimum thresholds were improved in low-frequency neurons from old mice treated with VGB (Fig. 4). The second is that there was a significant increase in the sound-evoked driven rate across all tonotopic regions (Fig. 5). Third, VGB improved symmetry in eFRAs from units in mid- and high-frequency tonotopic areas (Fig. 9). Finally, VGB treatment affected CF-dependent decreases in spontaneous rates (Fig. 10A). Previous research suggests that these effects should be attributable to VGB alone, as studies of long-term treatment with VGB demonstrated that there are no significant changes to alternative neuromodulatory systems (Ben-Menachem, 2011; Pitkänen et al., 1987; Sivenius et al., 1987). There have been reported increases in serotonin following VGB administration (Ben-Menachem et al., 1988), though this does not appear to be related to our results because it has been shown that direct administration of serotonin to IC neurons induced significant tone-evoked inhibition in 60%–80% of recorded neurons (Hurley and Pollak, 1999, 2001). This is in direct contrast to our results, which showed increases in driven rates to all tone-evoked frequencies.

Many studies have shown that GABA regulates inhibitory neurotransmission within the auditory system, we hypothesized that increasing available GABA within the synaptic cleft by irreversible inhibition of GABA transaminase would alter sound-evoked activity. A reduction in the levels of GABA within the auditory midbrain has been proposed as the underlying cause for the decrease in the percentage of units with nonmonotonic RIFs within the IC (Caspary et al., 1995; Willott et al., 1988a,b). This follows the same pattern of central gain control seen in maladaptive plasticity disorders such as tinnitus, where activity is increased in central auditory structures following reduced input from the cochlea and auditory nerve (Formby et al., 2007; Norena and Farley, 2013). In parallel, data from Leong et al. has shown that eFRAs had a higher asymmetry index and were broader in shape as animals aged (Leong et al., 2011). We found that treatment with VGB altered the shape of the eFRAs' in a positive manner, by increasing the symmetric structure of eFRAs found in middle-aged and young mice. In addition, VGB significantly increased tone-evoked RLFs, especially for moderate to intense stimuli, which could result in increased excitatory drive and improved salience of acoustic events.

Systemic administration of VGB in aged mice resulted in improved MTs for low-frequency units (dorsal), and conversely, poorer MTs in high CF units (ventral). This suggests that inhibition has divergent effects on near-threshold excitation, which may relate to the topographic differences in neurotransmitter expression. A similar finding was reported in a study of rats, which showed high variations in the number of GABA-positive neurons throughout the auditory midbrain and upper brainstem (Peruzzi et al., 1997). Although the decreases in GABA neurotransmission in the aged IC may be presumed to be the underlying cause of the increase in driven activity and MT improvements, the significant decreases in spontaneous activity across all frequency regions in our study indicate more complex

interactions exist. Previous studies of salicylate and pentobarbital, drugs known to modify GABA and alter both driven and spontaneous rates in rodents, demonstrated similar results of decreasing spontaneous rates in low-frequency IC units (Torterolo et al., 2002). Whole-cell recordings have also shown decreases in spontaneous activity, which was linked to increases in burst activity and hyperpolarization (Tan et al., 2007). However, compounds that increase available GABA can also alter spontaneous activity. When tiagabine, a GABA re-uptake inhibitor, was applied to hippocampal slices, spontaneous activity decreased over the course of 10 minutes (Leniger et al., 2000). This compound also acts more broadly on the GABAergic system than VGB, which is $GABA_A$ specific (Angehagen et al., 2003). We observed a significant increase in driven rates at moderate to high intensities (Figs. 5 and 9) for which repetitive bursting may have contributed. Repetitive firing or bursting at the onset of stimulation has been linked with low voltage–activated T-type Ca^{2+} channels (Cain and Snutch, 2013; Diana et al., 2007; Li et al., 2014; Oliver, 2005; Womack et al., 2004). Adding a T-type Ca^{2+} conductance to a model IC neuron also produced a rebound-sustained type of response (Rabang et al., 2012); however, this type of temporal response pattern was not common either before or after VGB administration.

Might changes in GABA receptors be associated with an overall change in the size of the IC? In a quantitative analysis of the aged IC in gerbils, Gleich et al. found that there was a small but significant decline in area of approximately 0.48 mm^2, which was unexpectedly accompanied by an increase in GABAergic cell levels (Gleich et al., 2014). In a contrasting study of an aging rat model, it was found that there were no significant differences in the total IC area, but an increase in the GABA γ_1 subunits and a decrease in the γ_2 subunits in the central IC (Caspary et al., 2008; Milbrandt et al., 1997) and AC (Caspary et al., 2013). Other studies have found varying proportions of GABA expression in the different tonotopic subdivisions of the IC, with larger proportions of GABA and glutamate decarboxylase seen in the dorsal (low frequency) region (Adams and Wenthold, 1979; Merchan et al., 2005). This distribution variance that occurs across different regions and species may explain the frequency-specific changes in asymmetry along with the changes in MTs, driven rates, and spontaneous rates mentioned previously. Whole-cell in vivo IC recordings have shown that the infusion of GABA antagonists significantly affects the discharge pattern and intensity of stimulus onset evoked spiking (Casseday et al., 2000). Other experimental results have revealed that characteristic excitability response differences exist between the somatic and dendritic regions of single neuronal cells following GABA manipulation (Breton and Stuart, 2012). Most of the studies which found an improvement in thresholds indicated that the loss of GABA allowed for the expansion of eFRA side bands via increases in driven spikes at increasing stimulus intensities in both the AC and IC (Calford et al., 1993; Caspary et al., 1995; Wang et al., 2000), these results may be modulated by GABA distribution through the different tonotopic regions of these auditory nuclei. However, our data indicate little variation in the type and sharpness (Q-values) of response properties (Fig. 8) with the increased availability of GABA, which may be attributed to a species specific or aging effect, as neither model has been thoroughly studied within the auditory midbrain of the mouse.

Previous studies have shown that age-related hearing loss often results in increases in both the thresholds and spontaneous activity within the dorsal nucleus of the lateral lemniscus

(NLL), IC, and AC. These changes are consistent with the observed decreases in salience following the induction of tinnitus (Kotak et al., 2005). The elevated thresholds of VGB-treated high-frequency units resemble shifts seen following noise and salicylate-induced tinnitus (Norena et al., 2010; Salvi et al., 2000). Such changes have been shown to increase the affinity of $GABA_A$ receptor binding sites (Milbrandt et al., 2000). In particular, they accompany layer-dependent changes in spontaneous firing rates within multiple auditory nuclei (Stolzberg et al., 2012). Treatment with VGB has been shown to eliminate the electrophysiological and behavioral markers associated with tinnitus following both acute treatment of sodium salicylate induced (Ma et al., 2006) and chronic treatment of noise-induced tinnitus (Chen and Jastreboff, 1995; Eggermont and Kenmochi, 1998; Ma et al., 2006; Muller et al., 2003; Stolzberg et al., 2012). Our study has shown that following systemic administration of VGB, there are both decreases in spontaneous activity and increases in the tone-evoked driven rates, which have the beneficial effects of increasing the signal-to-noise ratio. This may be the observed mechanism for the elimination of tinnitus discussed above.

Studies of the rat AC following treatment with salicylate from Stolzberg et al. found that results were often dependent on the location and CF and may be attributed to the salicylate acting directly in the central nervous system and not an effect of changes in GABAergic inhibition, as seen within this and other IC studies (Pollak and Park, 1993; Wang et al., 2000). Increases in sound-evoked spike, discharge rates have been observed following the blockage of local GABAergic circuits with bicuculline in the IC and AC (Pollak and Park, 1993; Wang et al., 2000). Our results showed amplified driven rates following GABA increases via the addition of VGB, which is somewhat paradoxical considering that it has been previously found that the addition of GABA to the IC decreased driven rates (Pollak and Park, 1993). However, the increases in driven rates we observed are similar to results seen in another lab when using the GABA agonist bicuculline (Backoff et al., 1999), which could indicate that GABAergic inhibition can work in different ways, as discussed above. We also found VGB-mediated increases in GABA significantly decreased spontaneous rates regardless of tonotopic area (Fig. 10A), similar to VGB-induced tinnitus treatment results seen behaviorally and within AI of the rat (Yang et al., 2011).

The VGB-induced reduction in the number of units with V-type receptive fields and the increase in the prevalence of primary-like eFRAs (Fig. 3) can be attributed to a weakening of inhibitory side bands which increased the overall area of the receptive field. Previous studies involving neurotransmitter expression and regulation of eFRAs were examined for equivalent comparisons in regard to modulation of the shape of the RF. These studies showed that modulation of the inhibitory receptive field is correlated to the location of GABA expression within the IC, with the strongest expression found in the dorsal-low frequency region (Adams and Wenthold, 1979; Oliver et al., 1994; Peruzzi et al., 1997). Our results showed increased driven rates within the eFRAs of aged animals following VGB-induced increases in GABA availability, whereas other labs found that blocking GABA receptor sites to increase available GABA in young healthy animals also increased driven rates, whereas the direct addition of more GABA depressed excitation (Mayko et al., 2012; Palombi and Caspary, 1996; Pollak and Park, 1993). Following the blockage of inhibitory sites, thresholds typically decreased, whereas the side bands of response areas increased

(Caspary et al., 2002; Palombi and Caspary, 1996), similar to our results in aged mice. Previously, the effects of modulating GABA were not well studied in aged animals, which are known to have depressed GABA expression. We have shown here that increasing the availability of GABA via the irreversible inhibition of GABA aminotransferase acts to both increase the driven firing rates within the RFs and decrease the spontaneous activity.

There are at least 2 possible mechanisms that could have the modulatory effects observed on neural activity after a systemic dose of VGB: (1) the observed effects could be inherited from the convergence of inhibitory inputs from caudal brainstem nuclei or (2) VGB-mediated intrinsic mechanisms may occur from interactions within the IC itself. While all subdivisions of the IC receive GABAergic inputs that come from a variety of sources, one of the largest GABAergic projections comes from the NLL (Kelly et al., 1998, 2009; Nakamoto et al., 2014). The NLL is a major source of GABAergic input to the IC from both binaural dorsal NLL (DNLL) and monaural ventral NLL pathways (Li and Kelly, 1992). If systemic VGB reduced the effective drive of DNLL neurons, this could release IC neurons from inhibition and result in an increase in driven activity. This possibility is supported by the findings of Kelly et al. where reducing the output of the DNLL via focal lesions increased driven activity recorded from the IC (Kelly et al., 1998; Li and Kelly, 1992). We also found that FSL was reduced following systemic VGB administration. Using whole-cell patch-clamp recordings from IC neurons in the bat, Covey et al. found that one-third of IC neurons received inhibitory postsynaptic currents at a much shorter latency then excitatory currents, which lengthen the response latency (Covey et al., 1996). Blocking GABAergic circuits has typically been shown to decrease FSL, indicating that the initial onset of the excitatory response may be reduced (Casseday et al., 2000; Pollak and Park, 1993). Again, a reduction in DNLL inhibitory drive could explain the underlying mechanism which resulted in the significantly reduced FSL seen in this study (Fig. 7).

Intrinsic mechanisms, via intra-lamina connections may also contribute, as GABAergic circuits in the IC are interconnected. Slice work in the mouse has shown that while a high percentage of recorded neurons received inputs from the NLL, they were also able to reduce GABAergic intra-neural responses via $GABA_A$ and glutamic neuromodulation. This resulted in complete abolishment of inhibitory postsynaptic potentials, while concurrently increasing excitatory postsynaptic potentials (Wagner, 1996). Research has also shown that adjacent neurons can receive very different inhibitory responses, with neighboring neurons responding contrarily to high- and low-frequency stimuli (Geis et al., 2011). This study found that while some units have highly correlated inputs, others showed similarity in the individual frequency response tuning curves or had overlapping eFRAs (Geis et al., 2011). It is possible that with multi-unit responses, we could be sampling data from 2 to 3 different neurons, which would include a significant number of inputs for both ipsi- and contra-lateral nuclei along with the intra-neuronal inhibitory events, which can converge on a neuronal cluster.

Before its inclusion in auditory research, VGB was primarily used as a treatment for epileptic seizures. Treatment was shown to elevate levels of GABA within hours of administration and offered partial protection from seizures, whereas plasma concentrations remained elevated between 1 week and 1 month (Petroff et al., 1999). However, one side-

effect of VGB treatment was visual field deficits in children due to irreversible atrophy of nerve fibers in the retina (Ben-Menachem, 2011; Frisen and Malmgren, 2003). VGB has been used to examine other aspects of auditory function, including the auditory-evoked potentials of dogs (Arezzo et al., 1989), where it created both inconsistent changes to the auditory brainstem response, and a significant increase in the latency of somatosensory-evoked potentials. VGB was also tested as a treatment for tinnitus, a disorder which makes localization difficult for patients with impaired temporal processing abilities (Zion Golumbic et al., 2012, 2013). One study found that VGB eliminated the behavioral evidence of noise-induced tinnitus in rats (Yang et al., 2011). Bauer et al. also found that VGB treatment reduced behavioral and electrophysiological evidence of noise-induced tinnitus, which subsequently returned after a washout period. They determined this was likely due to either decreases in GABA receptor binding sites or an increase in the afferent activity from the cochlea (Bauer et al., 2000). This study has shown VGB treatment in aged mice results in larger concentrations of GABA and has long lasting effects on neural responses recorded within the auditory midbrain, significantly increasing driven spike rates, improving minimum thresholds, and decreasing spontaneous activity in IC neurons.

In summary, this study found complex interactions in spectral processing following the increase of available GABA. While there have been various methods of increasing tone-evoked response rates, these improvements usually coincide with the loss of frequency-specific selectivity. Our results demonstrated that increasing GABA within the aged mouse IC via VGB administration decreased spontaneous activity and improved minimum thresholds, while maintaining frequency selectivity. Temporal processing is dependent on the auditory system's ability to prevent frequency masking of relevant auditory stimuli via inhibition of these errant stimuli. The increases in evoked firing, shifts in eFRAs, and decreased FSL are consistent with reductions in inhibition from caudal inputs; whereas declines in the rate of spontaneous activity are likely due to amplifications of laminar inhibition within the IC, which would thus act to modulate baseline excitation. Thus, the upregulation of GABA expression within the IC may contribute to preventing or minimizing the loss of hearing in noisy environments. This is due to the key role the IC plays in the coding and processing of sounds, which is highly dependent on inhibitory inputs. This study provides new understanding of the inhibitory neurotransmitter GABA and how it may contribute to overall auditory perception. These GABA-related improvements in neuronal frequency specificity through better MTs, increased driven rates, decreased spontaneous activity, and enhanced symmetry of eFRAs point to a potential mechanism for treating the speech recognition deficits that often occur with ARHL.

Acknowledgements

The authors would like to thank Dr. James Willott and Andrea Lowe, MS for their extensive review and editing of the manuscript. They would also like to thank the two anonymous reviewers for their time and critiques, as their contribution offered significant assistance in making this paper noteworthy.

References

Adams JC, Wenthold RJ, 1979 Distribution of putative amino acid transmitters, choline acetyltransferase and glutamate decarboxylase in the inferior colliculus. Neuroscience 4, 1947–1951. [PubMed: 231219]

Aitkin L, 1986 The inferior colliculus: nexus of the auditory pathway In: The Auditory Midbrain: Structure and Function in the Central Auditory Pathway. Humana, Clifton, NJ, pp. 75–100.

Allen PD, Eddins DA, 2010 Presbycusis phenotypes form a heterogeneous continuum when ordered by degree and configuration of hearing loss. Hear Res. 264, 10–20. [PubMed: 20144701]

Angehagen M, Ben-Menachem E, Ronnback L, Hansson E, 2003 Novel mechanisms of action of three antiepileptic drugs, vigabatrin, tiagabine, and topiramate. Neurochem. Res 28, 333–340. [PubMed: 12608706]

Arezzo JC, Schroeder CE, Litwak MS, Steward DL, 1989 Effects of vigabatrin on evoked potentials in dogs. Br. J. Clin. Pharmacol 27 (Suppl 1), 53S–60S. [PubMed: 2757910]

Arivazhagan P, Panneerselvam C, 2002 Neurochemical changes related to ageing in the rat brain and the effect of DL-alpha-lipoic acid. Exp. Gerontol 37, 1489–1494. [PubMed: 12559418]

Backoff PM, Shadduck Palombi P, Caspary DM, 1999 Gamma-aminobutyric acidergic and glycinergic inputs shape coding of amplitude modulation in the chinchilla cochlear nucleus. Hear Res. 134, 77–88. [PubMed: 10452378]

Barsz K, Ison JR, Snell KB, Walton JP, 2002 Behavioral and neural measures of auditory temporal acuity in aging humans and mice. Neurobiol. Aging 23, 565–578. [PubMed: 12009506]

Barsz K, Wilson WW, Walton JP, 2007 Reorganization of receptive fields following hearing loss in inferior colliculus neurons. Neuroscience 147, 532–545. [PubMed: 17540507]

Bauer CA, Brozoski TJ, Holder TM, Caspary DM, 2000 Effects of chronic salicylate on GABAergic activity in rat inferior colliculus. Hear Res. 147, 175–182. [PubMed: 10962183]

Ben-Menachem E, 2011 Mechanism of action of vigabatrin: correcting mis-perceptions. Acta Neurol. Scand. Suppl 124, 5–15.

Ben-Menachem E, Persson LI, Schechter PJ, Haegele KD, Huebert N, Hardenberg J, Dahlgren L, Mumford JP, 1988 Effects of single doses of vigabatrin on CSF concentrations of GABA, homocarnosine, homovanillic acid and 5-hydroxyindoleacetic acid in patients with complex partial epilepsy. Epilepsy Res. 2, 96–101. [PubMed: 3143561]

Ben-Menachem E, Sander JW, 2011 Vigabatrin therapy for refractory complex partial seizures: review of major European trials. Acta Neurol. Scand. Suppl 16–28. [PubMed: 22061177]

Breton JD, Stuart GJ, 2012 Somatic and dendritic GABA(B) receptors regulate neuronal excitability via different mechanisms. J. Neurophysiol 108, 2810–2818. [PubMed: 22956789]

Brimijoin WO, Walton JP, 2008 Aging affects the strength and frequency-dependence of a potential echo-suppression mechanism in the inferior colliculus. Paper Presented at the British Society of Audiology Annual Convention, London, UK.

Brozoski TJ, Spires TJ, Bauer CA, 2007 Vigabatrin, a GABA transaminase inhibitor, reversibly eliminates tinnitus in an animal model. J. Assoc. Res. Otolaryngol 8, 105–118. [PubMed: 17221143]

Cain SM, Snutch TP, 2013 T-type calcium channels in burst-firing, network synchrony, and epilepsy. Biochim. Biophys. Acta 1828, 1572–1578. [PubMed: 22885138]

Calford MB, Rajan R, Irvine DR, 1993 Rapid changes in the frequency tuning of neurons in cat auditory cortex resulting from pure-tone-induced temporary threshold shift. Neuroscience 55, 953–964. [PubMed: 8232905]

Caspary DM, Hughes LF, Ling LL, 2013 Age-related GABAA receptor changes in rat auditory cortex. Neurobiol. Aging 34, 1486–1496. [PubMed: 23257264]

Caspary DM, Ling L, Turner JG, Hughes LF, 2008 Inhibitory neurotransmission, plasticity and aging in the mammalian central auditory system. J. Exp. Biol 211 (Pt 11), 1781–1791. [PubMed: 18490394]

Caspary DM, Milbrandt JC, Helfert RH, 1995 Central auditory aging: GABA changes in the inferior colliculus. Exp. Gerontol 30, 349–360. [PubMed: 7556513]

Caspary DM, Palombi PS, Hughes LF, 2002 GABAergic inputs shape responses to amplitude modulated stimuli in the inferior colliculus. Hear Res. 168, 163–173. [PubMed: 12117518]

Casseday JH, Ehrlich D, Covey E, 2000 Neural measurement of sound duration: control by excitatory-inhibitory interactions in the inferior colliculus.J. Neurophysiol 84, 1475–1487. [PubMed: 10980020]

Cheeseman P, Stutz J, 1996 Bayesian classification (AutoClass): theory and results, in Advances in knowledge discovery and data mining. In: Usama MF, et al. (Eds.), American Association for Artificial Intelligence, pp. 153–180.

Chen GD, Jastreboff PJ, 1995 Salicylate-induced abnormal activity in the inferior colliculus of rats. Hear Res. 82, 158–178. [PubMed: 7775282]

Covey E, Casseday JH, 1999 Timing in the auditory system of the bat. Annu. Rev. Physiol 61, 457–476. [PubMed: 10099697]

Covey E, Kauer JA, Casseday JH, 1996 Whole-cell patch-clamp recording reveals subthreshold sound-evoked postsynaptic currents in the inferior colliculus of awake bats. J. Neurosci 16, 3009–3018. [PubMed: 8622130]

Diana MA, Otsu Y, Maton G, Collin T, Chat M, Dieudonne S, 2007 T-type and L-type Ca2+ conductances define and encode the bimodal firing pattern of vestibulocerebellar unipolar brush cells. J. Neurosci 27, 3823–3838. [PubMed: 17409247]

Eggermont JJ, Kenmochi M, 1998 Salicylate and quinine selectively increase spontaneous firing rates in secondary auditory cortex. Hear Res. 117, 149–160. [PubMed: 9557985]

Engineer ND, Percaccio CR, Pandya PK, Moucha R, Rathbun DL, Kilgard MP, 2004 Environmental enrichment improves response strength, threshold, selectivity, and latency of auditory cortex neurons. J. Neurophysiol 92, 73–82. [PubMed: 15014105]

Faingold CL, 2002 Role of GABA abnormalities in the inferior colliculus pathophysiology—audiogenic seizures. Hear Res. 168, 223–237. [PubMed: 12117523]

Faingold CL, Boersma Anderson CA, Caspary DM, 1991 Involvement of GABA in acoustically-evoked inhibition in inferior colliculus neurons. Hear Res. 52, 201–216. [PubMed: 2061208]

Faingold CL, Gehlbach G, Caspary DM, 1989 On the role of GABA as an inhibitory neurotransmitter in inferior colliculus neurons—iontophoretic studies. Brain Res. 500, 302–312. [PubMed: 2605499]

Faingold CL, Li Y, Evans MS, 2000 Decreased GABA and increased glutamate receptor-mediated activity on inferior colliculus neurons in vitro are associated with susceptibility to ethanol withdrawal seizures. Brain Res. 868, 287–295. [PubMed: 10854581]

Formby C, Sherlock L, Gold S, Hawley M, 2007 Adaptive recalibration of chronic auditory gain. Semin. Hear 28, 295–302.

Frisen L, Malmgren K, 2003 Characterization of vigabatrin-associated optic atrophy. Acta Ophthalmol. Scand 81, 466–473. [PubMed: 14510793]

Frisina DR, Frisina RD, 1997 Speech recognition in noise and presbycusis: relations to possible neural mechanisms. Hear Res. 106, 95–104. [PubMed: 9112109]

Frisina RD, Walton JP, 2001a Aging of the mouse central auditory system In: Willott JF (Ed.), Handbook of Mouse Auditory Research: From Behavior to Molecular Biology. CRC Press, New York, pp. 339–379.

Frisina RD, Walton JP, 2001b Neuroanatomy of the central auditory system In: Willott JF (Ed.), Handbook of Mouse Auditory Research: From Behavior to Molecular Biology. CRC Press, New York, pp. 243–275.

Geis HR, van der Heijden M, Borst JG, 2011 Subcortical input heterogeneity in the mouse inferior colliculus. J. Physiol 589 (Pt 16), 3955–3967. [PubMed: 21727222]

Gleich O, Hamann I, Klump GM, Kittel M, Strutz J, 2003 Boosting GABA improves impaired auditory temporal resolution in the gerbil. Neuroreport 14, 1877–1880. [PubMed: 14534439]

Gleich O, Netz J, Strutz J, 2014 Comparing the inferior colliculus of young and old gerbils (Meriones unguiculatus) with an emphasis on GABA. Exp. Gerontol 57, 155–162. [PubMed: 24879972]

Gleich O, Strutz J, 2011 The effect of gabapentin on gap detection and forward masking in young and old gerbils. Ear Hear 32, 741–749. [PubMed: 21730860]

Gram L, Larsson OM, Johnsen A, Schousboe A, 1989 Experimental studies of the influence of vigabatrin on the GABA system. Br. J. Clin. Pharmacol 27 (Suppl 1), 13S–17S. [PubMed: 2757904]

Grose JH, Mamo SK, 2010 Processing of temporal fine structure as a function of age. Ear Hear 31, 755–760. [PubMed: 20592614]

Helfert RH, Glatz FR, 3rd, Wilson TS, Ramkumar V, Hughes LF, 2002 Hsp70 in the inferior colliculus of Fischer-344 rats: effects of age and acoustic stress. Hear Res. 170, 155–165. [PubMed: 12208549]

Helfert RH, Krenning J, Wilson TS, Hughes LF, 2003 Age-related synaptic changes in the anteroventral cochlear nucleus of Fischer-344 rats. Hear Res. 183, 18–28. [PubMed: 13679134]

Henry KR, Chole RA, 1980 Genotypic differences in behavioral, physiological and anatomical expressions of age-related hearing loss in the laboratory mouse: original papers travaux originaux. Audiology 19, 369–383. [PubMed: 7436856]

Hernandez O, Espinosa N, Perez-Gonzalez D, Malmierca MS, 2005 The inferior colliculus of the rat: a quantitative analysis of monaural frequency response areas. Neuroscience 132, 203–217. [PubMed: 15780479]

Herrmann B, Parthasarathy A, Han EX, Obleser J, Bartlett EL, 2015 Sensitivity of rat inferior colliculus neurons to frequency distributions. J. Neurophysiol 114, 2941–2954. [PubMed: 26354316]

Hurley LM, Pollak GD, 1999 Serotonin differentially modulates responses to tones and frequency-modulated sweeps in the inferior colliculus. J. Neurosci 19, 8071–8082. [PubMed: 10479707]

Hurley LM, Pollak GD, 2001 Serotonin effects on frequency tuning of inferior colliculus neurons. J. Neurophysiol 85, 828–842. [PubMed: 11160516]

Johannessen SI, Tomson T, 2006 Pharmacokinetic variability of newer antiepileptic drugs: when is monitoring needed? Clin. Pharmacokinet 45, 1061–1075. [PubMed: 17048972]

Kelly JB, Liscum A, van Adel B, Ito M, 1998 Projections from the superior olive and lateral lemniscus to tonotopic regions of the rat's inferior colliculus. Hear Res. 116, 43–54. [PubMed: 9508027]

Kelly JB, van Adel BA, Ito M, 2009 Anatomical projections of the nuclei of the lateral lemniscus in the albino rat (Rattus norvegicus). J. Comp. Neurol 512, 573–593. [PubMed: 19034907]

Kirby AE, Middlebrooks JC, 2012 Unanesthetized auditory cortex exhibits multiple codes for gaps in cochlear implant pulse trains. J. Assoc. Res. Otolaryngol 13, 67–80. [PubMed: 21969022]

Kotak VC, Fujisawa S, Lee FA, Karthikeyan O, Aoki C, Sanes DH, 2005 Hearing loss raises excitability in the auditory cortex. J. Neurosci 25, 3908–3918. [PubMed: 15829643]

Leniger T, Wiemann M, Bingmann D, Hufnagel A, Bonnet U, 2000 Different effects of GABAergic anticonvulsants on 4-aminopyridine-induced spontaneous GABAergic hyperpolarizations of hippocampal pyramidal cells–implication for their potency in migraine therapy. Cephalalgia 20, 533–537. [PubMed: 11075835]

Leong UC, Barsz K, Allen PD, Walton JP, 2011 Neural correlates of age-related declines in frequency selectivity in the auditory midbrain. Neurobiol. Aging 32, 168–178. [PubMed: 19246123]

Li HS, Borg E, 1991 Age-related loss of auditory sensitivity in two mouse geno-types. Acta Otolaryngol. 111, 827–834. [PubMed: 1759567]

Li L, Kelly JB, 1992 Inhibitory influence of the dorsal nucleus of the lateral lemniscus on binaural responses in the rat's inferior colliculus. J. Neurosci 12, 4530–4539. [PubMed: 1432109]

Li Y, Davey RA, Sivaramakrishnan S, Lynch WP, 2014 Postinhibitory rebound neurons and networks are disrupted in retrovirus-induced spongiform neuro-degeneration. J. Neurophysiol 112, 683–704. [PubMed: 25252336]

Llano DA, Turner J, Caspary DM, 2012 Diminished cortical inhibition in an aging mouse model of chronic tinnitus. J. Neurosci 32, 16141–16148. [PubMed: 23152598]

Ma WL, Hidaka H, May BJ, 2006 Spontaneous activity in the inferior colliculus of CBA/J mice after manipulations that induce tinnitus. Hear Res. 212, 9–21. [PubMed: 16307852]

Mattson RH, Petroff OA, Rothman D, Behar K, 1995 Vigabatrin: effect on brain GABA levels measured by nuclear magnetic resonance spectroscopy. Acta Neurol. Scand. Suppl 162, 27–30. [PubMed: 7495186]

Mayko ZM, Roberts PD, Portfors CV, 2012 Inhibition shapes selectivity to vocalizations in the inferior colliculus of awake mice. Front Neural. Circuits 6, 73. [PubMed: 23087616]

Merchan M, Aguilar LA, Lopez-Poveda EA, Malmierca MS, 2005 The inferior colliculus of the rat: quantitative immunocytochemical study of GABA and glycine. Neuroscience 136, 907–925. [PubMed: 16344160]

Milbrandt JC, Holder TM, Wilson MC, Salvi RJ, Caspary DM, 2000 GAD levels and muscimol binding in rat inferior colliculus following acoustic trauma. Hear Res. 147, 251–260. [PubMed: 10962189]

Milbrandt JC, Hunter C, Caspary DM, 1997 Alterations of GABAA receptor subunit mRNA levels in the aging Fischer 344 rat inferior colliculus. J. Comp. Neurol 379, 455–465. [PubMed: 9067836]

Mossop JE, Wilson MJ, Caspary DM, Moore DR, 2000 Down-regulation of inhibition following unilateral deafening. Hear Res. 147, 183–187. [PubMed: 10962184]

Muller M, Klinke R, Arnold W, Oestreicher E, 2003 Auditory nerve fibre responses to salicylate revisited. Hear Res. 183, 37–43. [PubMed: 13679136]

Nakamoto KT, Mellott JG, Killius J, Storey-Workley ME, Sowick CS, Schofield BR, 2014 Ultrastructural characterization of GABAergic and excitatory synapses in the inferior colliculus. Front Neuroanat. 8, 108. [PubMed: 25400551]

Norena AJ, Farley BJ, 2013 Tinnitus-related neural activity: theories of generation, propagation, and centralization. Hear Res. 295, 161–171. [PubMed: 23088832]

Norena AJ, Moffat G, Blanc JL, Pezard L, Cazals Y, 2010 Neural changes in the auditory cortex of awake Guinea pigs after two tinnitus inducers: salicylate and acoustic trauma. Neuroscience 166, 1194–1209. [PubMed: 20096752]

Ohlemiller KK, Dahl AR, Gagnon PM, 2010 Divergent aging characteristics in CBA/J and CBA/CaJ mouse cochleae. J. Assoc. Res. Otolaryngol 11, 605–623. [PubMed: 20706857]

Ohlemiller KK, Frisina RD, 2008 Age-Related Hearing Loss and its cellular and molecular bases In: Schacht J, Popper AN, Fay RR (Eds.), Auditory Trauma, Protection, and Repair, Vol. 31 Springer, US, pp. 145–194.

Oliver DL, 2005 Neuronal organization in the inferior colliculus In: Winer JA, Schreiner CE (Eds.), The Inferior Colliculus. Springer New York, New York, NY, pp. 69–114.

Oliver DL, Winer JA, Beckius GE, Saint Marie RL, 1994 Morphology of GABAergic neurons in the inferior colliculus of the cat. J. Comp. Neurol 340, 27–42. [PubMed: 7909821]

Palmer AR, Shackleton TM, Sumner CJ, Zobay O, Rees A, 2013 Classification of frequency response areas in the inferior colliculus reveals continua not discrete classes. J. Physiol 591, 4003–4025. [PubMed: 23753527]

Palombi PS, Caspary DM, 1996 GABA inputs control discharge rate primarily within frequency receptive fields of inferior colliculus neurons. J. Neurophysiol 75, 2211–2219. [PubMed: 8793735]

Parthasarathy A, Bartlett EL, 2011 Age-related auditory deficits in temporal processing in F-344 rats. Neuroscience 192, 619–630. [PubMed: 21723376]

Parthasarathy A, Cunningham PA, Bartlett EL, 2010 Age-related differences in auditory processing as assessed by amplitude-modulation following responses in quiet and in noise. Front Aging Neurosci. 2, 152. [PubMed: 21188162]

Paxinos G, Franklin KBJ, 2001 The Mouse Brain in Stereotaxic Coordinates, second ed Elsevier Academic Press, San Diego, CA.

Pedemonte M, Torterolo P, Velluti RA, 1997 In vivo intracellular characteristics of inferior colliculus neurons in Guinea pigs. Brain Res. 759, 24–31. [PubMed: 9219859]

Peruzzi D, Bartlett E, Smith PH, Oliver DL, 1997 A monosynaptic GABAergic input from the inferior colliculus to the medial geniculate body in rat.J. Neurosci 17, 3766–3777. [PubMed: 9133396]

Petroff OA, Hyder F, Collins T, Mattson RH, Rothman DL, 1999 Acute effects of vigabatrin on brain GABA and homocarnosine in patients with complex partial seizures. Epilepsia 40, 958–964. [PubMed: 10403220]

Pitkänen A, Halonen T, Ylinen A, Riekkinen P, 1987 Somatostatin, β-endorphin, and prolactin levels in human cerebrospinal fluid during the γ-vinyl-GABA treatment of patients with complex partial epilepsy. Neuropeptides 9, 185–195. [PubMed: 2885776]

Pollak GD, Park TJ, 1993 The effects of GABAergic inhibition on monaural response properties of neurons in the mustache bat's inferior colliculus. Hear Res. 65, 99–117. [PubMed: 8384613]

Rabang CF, Parthasarathy A, Venkataraman Y, Fisher ZL, Gardner SM, Bartlett EL, 2012 A computational model of inferior colliculus responses to amplitude modulated sounds in young and aged rats. Front Neural. Circuits 6, 77. [PubMed: 23129994]

Rees A, Moller AR, 1983 Responses of neurons in the inferior colliculus of the rat to AM and FM tones. Hear Res. 10, 301–330. [PubMed: 6874603]

Rees A, Moller AR, 1987 Stimulus properties influencing the responses of inferior colliculus neurons to amplitude-modulated sounds. Hear Res. 27, 129–143. [PubMed: 3610842]

Rey E, Pons G, Olive G, 1992 Vigabatrin. Clinical pharmacokinetics. Clin. Pharmacokinet 23, 267–278. [PubMed: 1395360]

Salvi RJ, Wang J, Ding D, 2000 Auditory plasticity and hyperactivity following cochlear damage. Hear Res. 147, 261–274. [PubMed: 10962190]

Shaddock Palombi P, Backoff PM, Caspary DM, 2001 Responses of young and aged rat inferior colliculus neurons to sinusoidally amplitude modulated stimuli. Hear Res. 153, 174–180. [PubMed: 11223307]

Sivenius MR, Ylinen A, Murros K, Matilainen R, Riekkinen P, 1987 Double-blind dose reduction study of vigabatrin in complex partial epilepsy. Epilepsia 28, 688–692. [PubMed: 3319536]

Spongr VP, Flood DG, Frisina RD, Salvi RJ, 1997 Quantitative measures of hair cell loss in CBA and C57BL/6 mice throughout their life spans. J. Acoust. Soc. Am 101, 3546–3553. [PubMed: 9193043]

Stiebler I, 1986 Tone-threshold mapping in the inferior colliculus of the house mouse. Neurosci. Lett 65, 336–340. [PubMed: 3520399]

Stiebler I, Ehret G, 1985 Inferior colliculus of the house mouse. I. A quantitative study of tonotopic organization, frequency representation, and tone-threshold distribution. J. Comp. Neurol 238, 65–76. [PubMed: 4044904]

Stolzberg D, Chrostowski M, Salvi RJ, Allman BL, 2012 Intracortical circuits amplify sound-evoked activity in primary auditory cortex following systemic injection of salicylate in the rat. J. Neurophysiol 108, 200–214. [PubMed: 22496535]

Stutz J, Cheeseman P, 1996 Autoclass—A Bayesian Approach to Classification. In: Skilling J, Sibisi S (Eds.). Springer, Netherlands.

Sutter ML, 2000 Shapes and level tolerances of frequency tuning curves in primary auditory cortex: quantitative measures and population codes. J. Neurophysiol 84, 1012–1025. [PubMed: 10938324]

Tan ML, Theeuwes HP, Feenstra L, Borst JG, 2007 Membrane properties and firing patterns of inferior colliculus neurons: an in vivo patch-clamp study in rodents. J. Neurophysiol 98, 443–453. [PubMed: 17507499]

Torterolo P, Falconi A, Morales-Cobas G, Velluti RA, 2002 Inferior colliculus unitary activity in wakefulness, sleep and under barbiturates. Brain Res. 935, 9–15. [PubMed: 12062467]

Turner JG, Hughes LF, Caspary DM, 2005a Affects of aging on receptive fields in rat primary auditory cortex layer V neurons. J. Neurophysiol 94, 2738–2747. [PubMed: 16000522]

Turner JG, Hughes LF, Caspary DM, 2005b Divergent response properties of layer-V neurons in rat primary auditory cortex. Hear Res. 202, 129–140. [PubMed: 15811705]

Turner JG, Parrish JL, Zuiderveld L, Darr S, Hughes LF, Caspary DM, Idrezbegovic E, Canlon B, 2013 Acoustic experience alters the aged auditory system. Ear Hear 34, 151–159. [PubMed: 23086424]

Wagner T, 1996 Lemniscal input to identified neurons of the central nucleus of mouse inferior colliculus: an intracellular brain slice study. Eur. J. Neurosci 8, 1231–1239. [PubMed: 8752593]

Walton JP, Barsz K, Wilson WW, 2008 Sensorineural hearing loss and neural correlates of temporal acuity in the inferior colliculus of the C57BL/6 mouse. J. Assoc. Res. Otolaryngol 9, 90–101. [PubMed: 17994264]

Walton JP, Frisina RD, O'Neill WE, 1998 Age-related alteration in processing of temporal sound features in the auditory midbrain of the CBA mouse. J. Neurosci 18, 2764–2776. [PubMed: 9502833]

Wang J, Caspary D, Salvi RJ, 2000 GABA-A antagonist causes dramatic expansion of tuning in primary auditory cortex. Neuroreport 11, 1137–1140. [PubMed: 10790896]

Willott JF, Kulig J, Satterfield T, 1984 The acoustic startle response in DBA/2 and C57BL/6 mice: relationship to auditory neuronal response properties and hearing impairment. Hear Res. 16, 161–167. [PubMed: 6526747]

Willott JF, Pankow D, Hunter KP, Kordyban M, 1985 Projections from the anterior ventral cochlear nucleus to the central nucleus of the inferior colliculus in young and aging C57BL/6 mice. J. Comp. Neurol 237, 545–551. [PubMed: 3840181]

Willott JF, Parham K, Hunter KP, 1988a Response properties of inferior colliculus neurons in middle-aged C57BL/6J mice with presbycusis. Hear Res. 37, 15–27. [PubMed: 3225229]

Willott JF, Parham K, Hunter KP, 1988b Response properties of inferior colliculus neurons in young and very old Cba/J mice. Hear Res. 37, 1–14. [PubMed: 3225228]

Willott JF, Parham K, Hunter KP, 1991 Comparison of the auditory sensitivity of neurons in the cochlear nucleus and inferior colliculus of young and aging C57BL/6J and CBA/J mice. Hear Res. 53, 78–94. [PubMed: 2066290]

Womack MD, Chevez C, Khodakhah K, 2004 Calcium-activated potassium channels are selectively coupled to P/Q-type calcium channels in cerebellar Purkinje neurons. J. Neurosci 24, 8818–8822. [PubMed: 15470147]

Yan J, Zhang Y, Ehret G, 2005 Corticofugal shaping of frequency tuning curves in the central nucleus of the inferior colliculus of mice. J. Neurophysiol 93, 71–83. [PubMed: 15331615]

Yang S, Weiner BD, Zhang LS, Cho SJ, Bao S, 2011 Homeostatic plasticity drives tinnitus perception in an animal model. Proc. Natl. Acad. Sci. U. S. A 108, 14974–14979. [PubMed: 21896771]

Zion Golumbic EM, Ding N, Bickel S, Lakatos P, Schevon CA, McKhann GM, Goodman RR, Emerson R, Mehta AD, Simon JZ, Poeppel D, Schroeder CE, 2013 Mechanisms underlying selective neuronal tracking of attended speech at a “cocktail party”. Neuron 77, 980–991. [PubMed: 23473326]

Zion Golumbic EM, Poeppel D, Schroeder CE, 2012 Temporal context in speech processing and attentional stream selection: a behavioral and neural perspective. Brain Lang. 122, 151–161. [PubMed: 22285024]

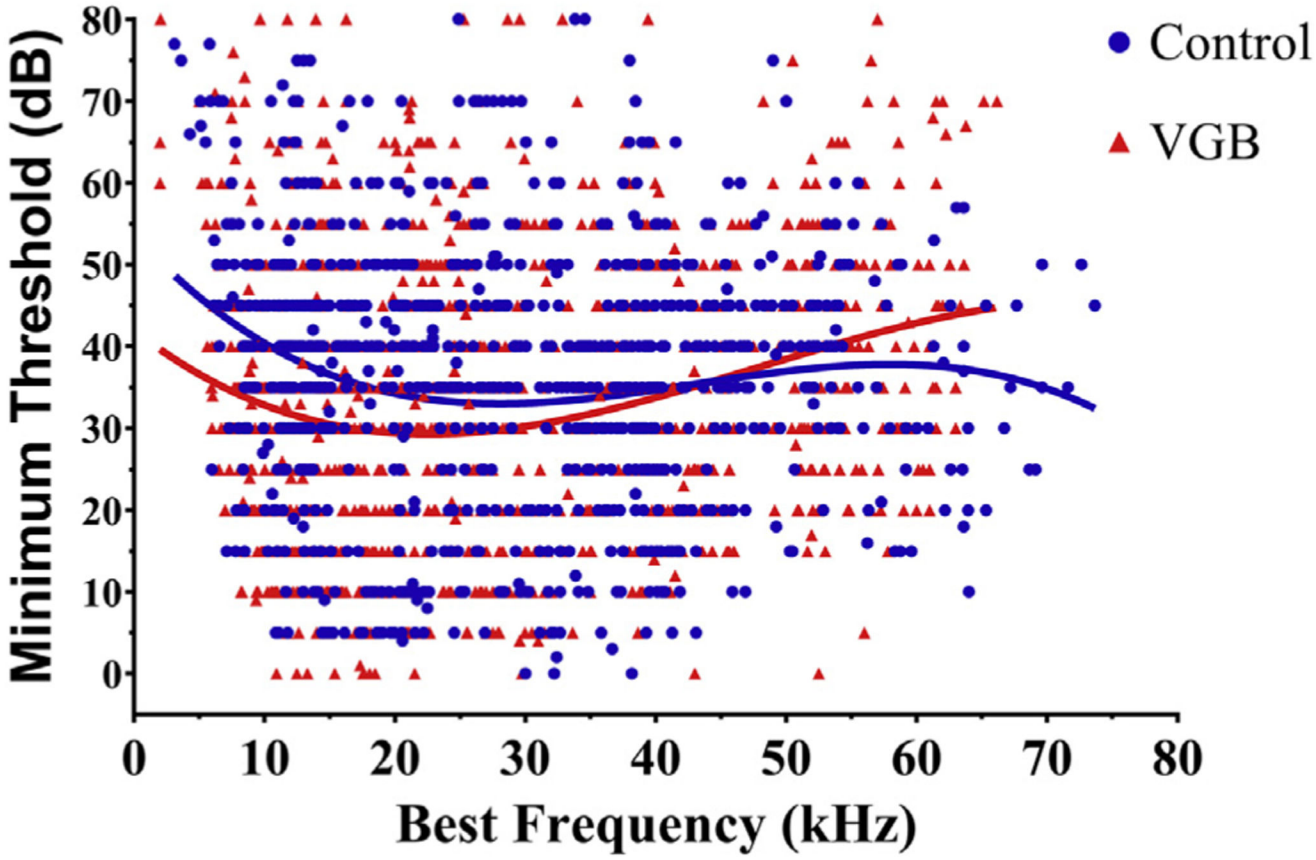

Fig. 1.

Best frequency versus minimum threshold. Overall distribution of all recorded units (492 control and 495 VGB treated) from 43 old CBA/CaJ mice. Mean minimum thresholds (MTs) were significantly lower for VGB-treated units from the low-tonotopic region and were higher in units from the high-frequency region. No significant differences were seen for mid-range units. Abbreviation: VGB, vigabatrin.

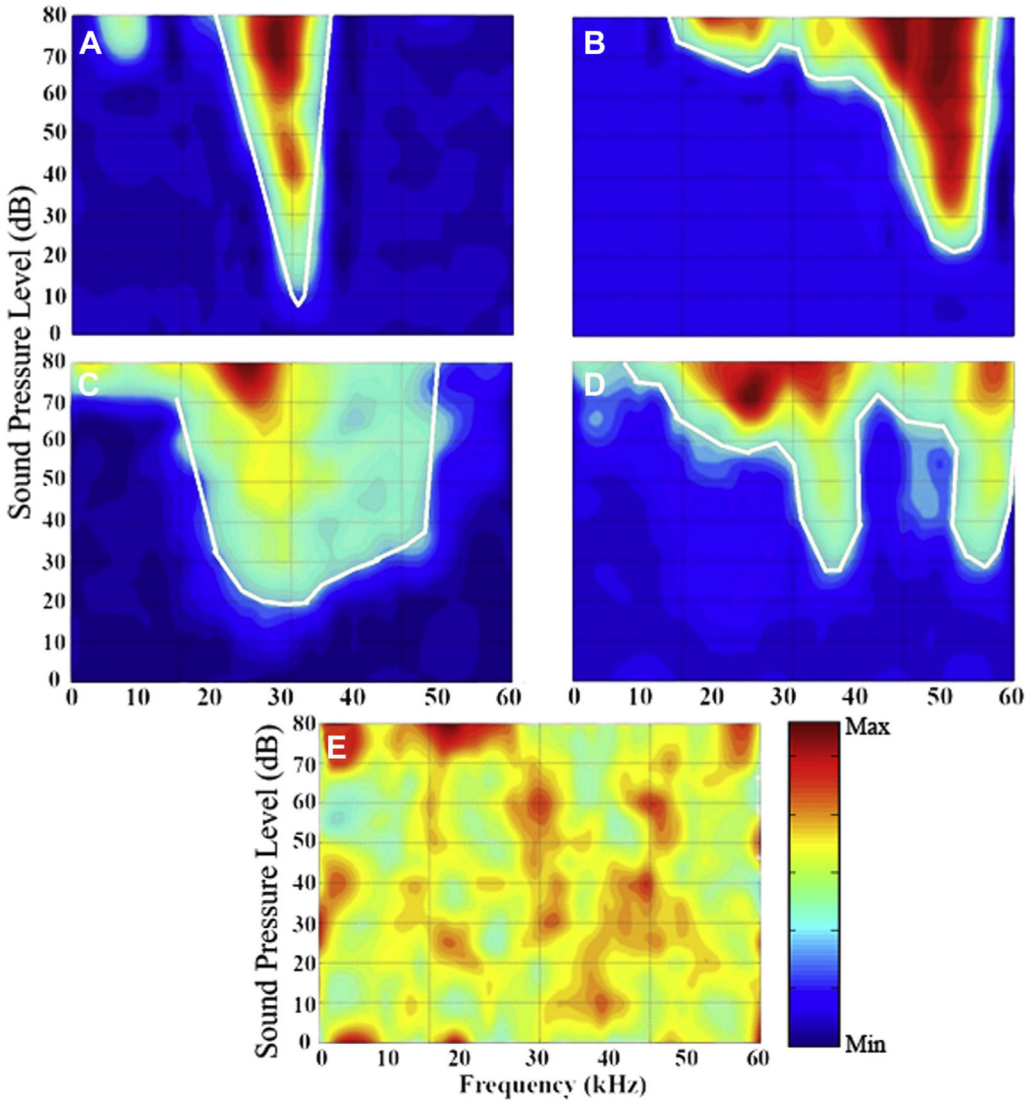

Fig. 2.

Various types of eFRAs that were recorded in both the treated and control mice. Representative examples of eFRAs are shown with sound intensity plotted as a function of frequency, and the number of spikes represented by the color map. Regions of low sound–evoked neural activity are represented as blue, and high spiking activity as red. (A) The V-type eFRA which is the most prominent type observed within the mouse IC and has steep low and high-frequency slopes on either side of the best frequency. (B) Primary-like eFRA, which consists of a sharp HF edge and shallow LF edge, with the addition of an LF tail. (C) The U-type eFRA, which has similar characteristics to the V-type, but responds to a broader range of frequencies near threshold. (D) The multi-peaked eFRA type, which has 2 tuned excitatory areas separated by a nonresponsive region. (E) A closed-complex eFRA, which is comprised of a diffuse area of responsiveness and frequently has an enclosed excitatory region and high spontaneous activity. Abbreviations: eFRA, excitatory frequency response areas; HF, high frequency; IC, colliculus; LF, low frequency. (For interpretation of the

references to color in this figure legend, the reader is referred to the Web version of this article.)

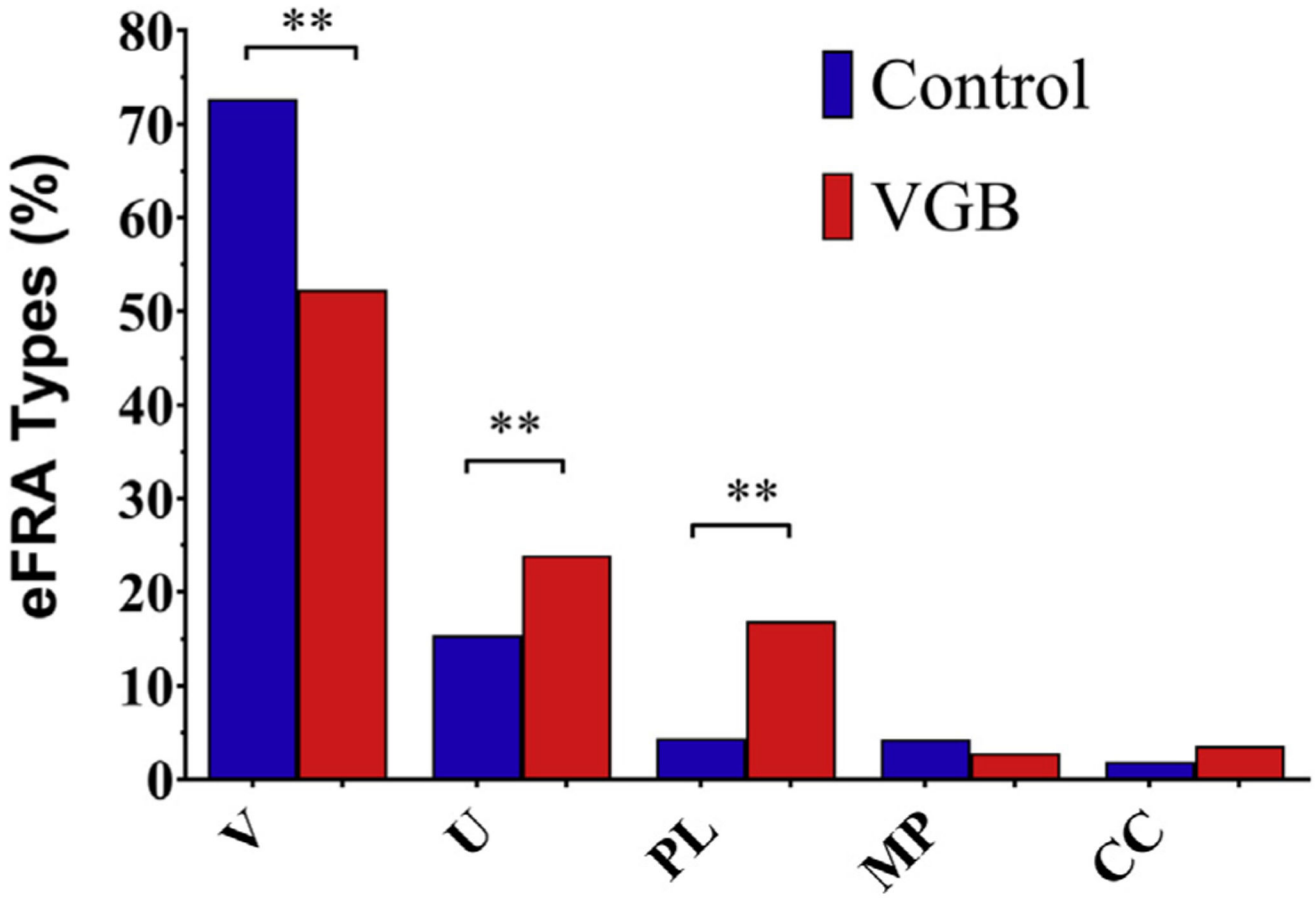

Fig. 3.

Distribution of the proportion of eFRA types found in control (blue) and VGB-treated (red) animals. The abcissa indicates the 5 types of the eFRAs shown in Fig. 2: V-shaped (V), U-shaped (U), primary-like (PL), multi-peak (MP), and closed-complex (CC). There was an overall effect of treatment, with v-type, u-type, and primary-like units showing significant differences following post hoc testing ($^{**}p < 0.01$). The distribution of multi-peaked and closed-complex eFRAs types were similar between the 2 groups. Abbreviation: VGB, vigabatrin. (For interpretation of the references to color in this figure legend, the reader is referred to the Web version of this article.)

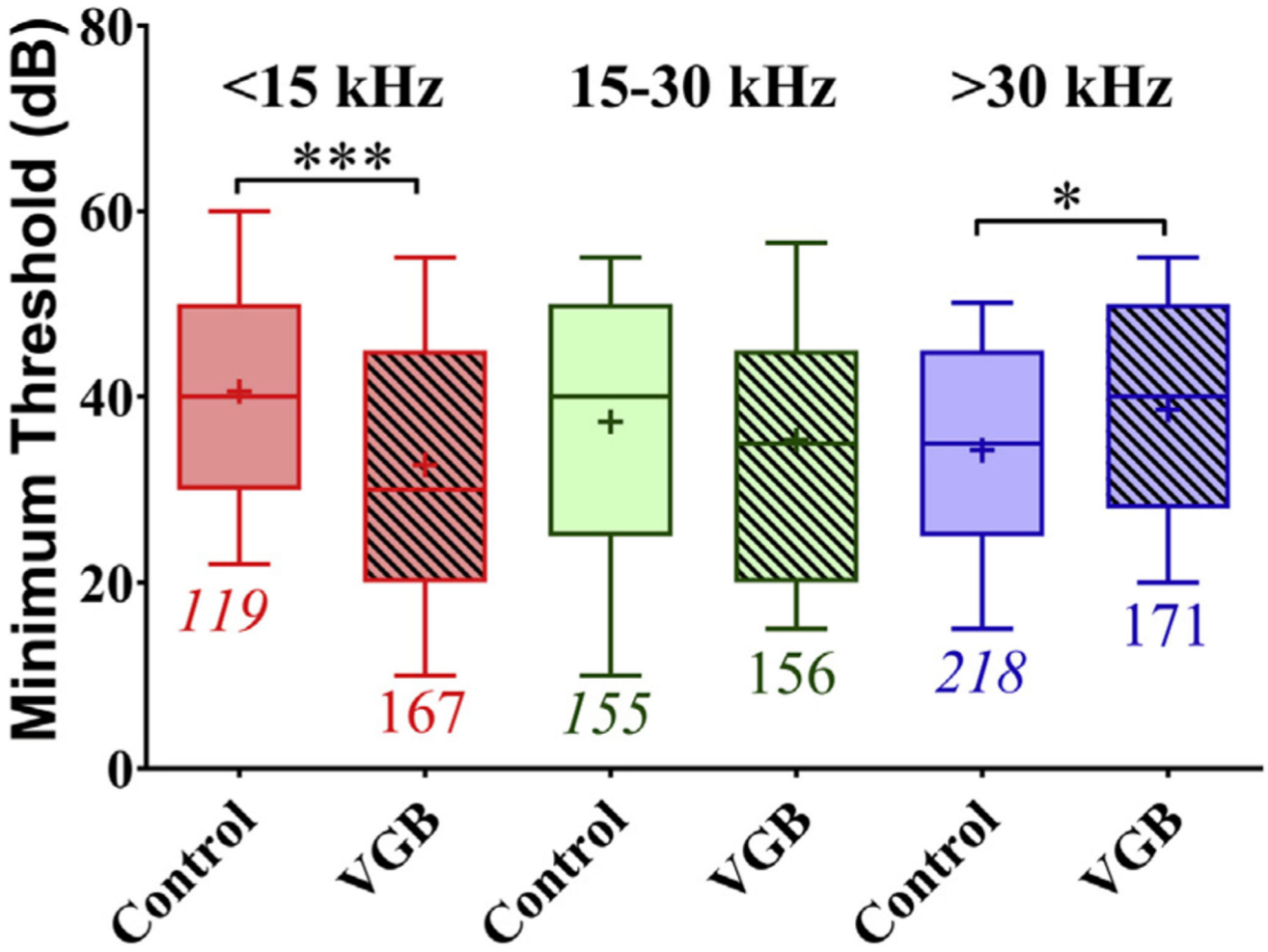

Fig. 4.

Minimum thresholds of control and treated units plotted as a function of tonotopic regions. In the LF (<15 kHz) region, the mean minimum threshold was significantly lower in units from treated mice ($^{***}p = 0.002$). No significant differences in MTs following VGB were observed for units with mid-range CFs (15–30 kHz). However, in the HF (>30 kHz) tonotopic region, MTs were higher in the VGB units ($^{*}p < 0.05$). These results demonstrate that the greatest effect on threshold following VGB treatment was found in the dorsal, low-frequency region of the IC. Abbreviations: CFs, characteristic frequencies; IC, colliculus; LF, low frequency; MTs, minimum thresholds; VGB, vigabatrin.

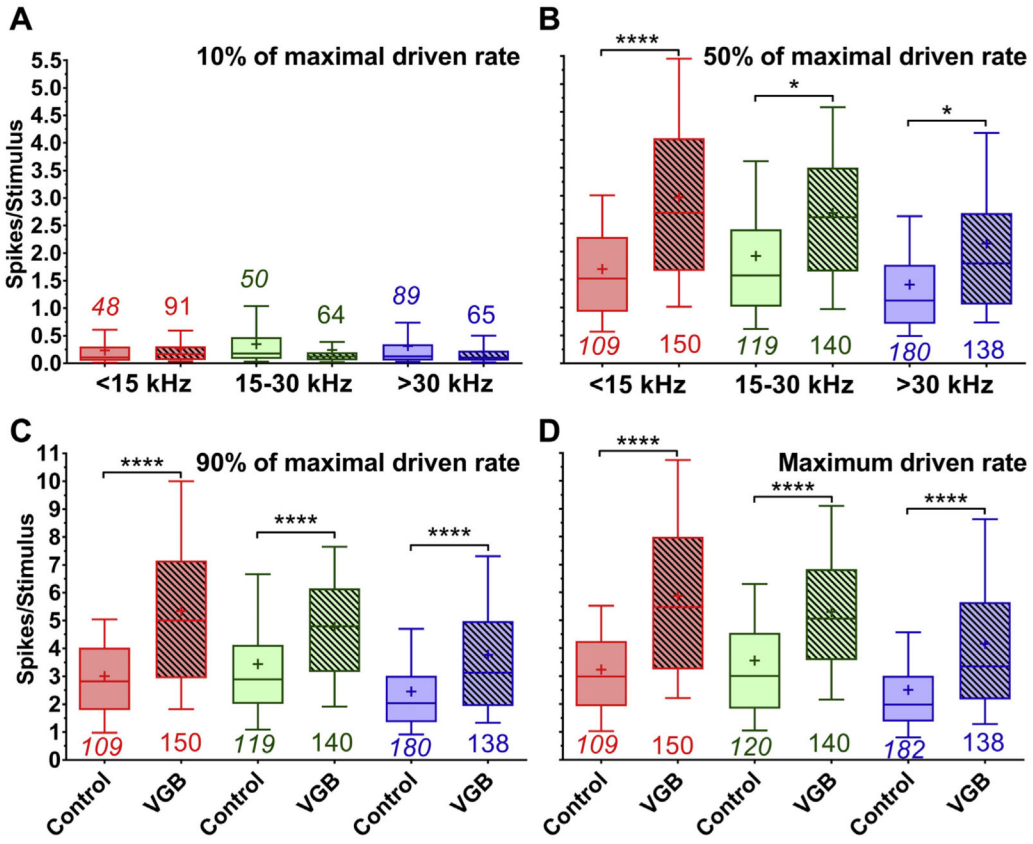

Fig. 5.

Mean spike counts of control and VGB-treated units taken from RLFs derived from the BF of the eFRA and shown for the 10%, 50%, 90%, and maximum driven rate taken from eFRAs. Spike counts were derived from the 10%, 50%, 90%, and maximum driven rates points from tone RLFs measured in a 25 ms window and subdivided into low-, mid-, and high-frequency regions. There was an overall effect of treatment and tonotopic region, with several post hoc significant differences ($^{****}p < 0.0001$, $^{*}p < 0.05$). The mean spike counts at 10% for the control and VGB-driven units (A) during eFRAs demonstrated no significant effects of treatment. There was a significant increase in mean spike counts for VGB-treated units at the 50% point (B) on the RLF, which was observed for all tonotopic regions. This increase in sound-evoked activity in the eFRA was also observed for the mean spike counts at 90% (C) across all tonotopic subdivisions. Maximum spike counts (D) were also significantly higher in units from mice treated with VGB as compared with control mice across all frequency regions. Abbreviations: BF, best frequency; eFRA, excitatory frequency response areas; RLF, rate-level function; VGB, vigabatrin.

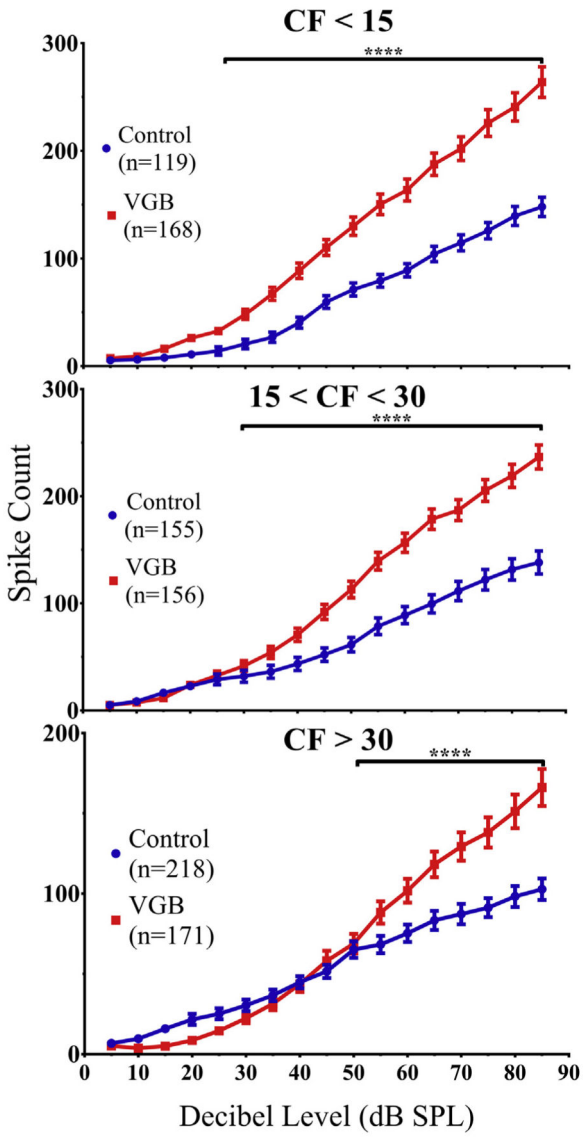

Fig. 6.

Average RLF population functions were altered by VGB treatment in all 3 tonotopic regions in an intensity-dependent manner. There was a significant divergence in the population RLFs depending on the tonotopic subregion, this occurred in responses to stimuli above 25 dB for units with CFs <15 kHz, above 30 dB for mid-frequency CFs, and above 50 dB for units with CFs >30 kHz ($^{****}p < 0.0001$). In addition, units from all 3 frequency regions from VGB-treated mice exhibited steeper slopes. In parallel with the threshold results seen in Fig. 4, there was a reduction in responses to lower intensity sounds for the high-frequency region and an enhancement within the low-frequency region. Abbreviations: CFs, characteristic frequencies; eFRA, excitatory frequency response areas; RLF, rate-level function; VGB, vigabatrin.

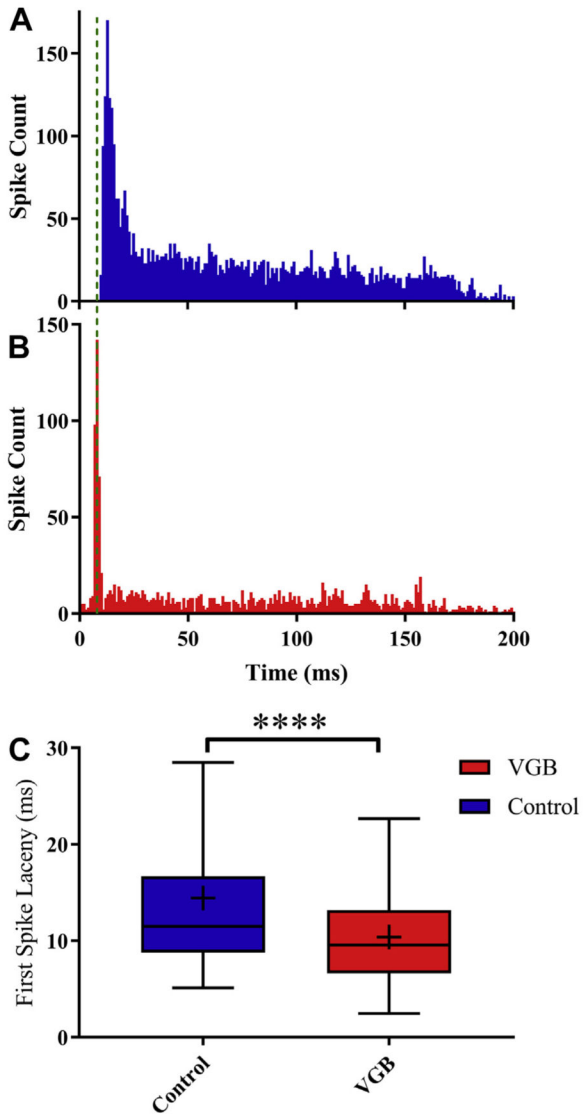

Fig. 7.

Systemic administration of VGB shortens the first spike latency of onset neurons. FSL was measured from post-stimulus time spike latencies elicited by a 70 dB SPL broadband noise burst. (A) A representative PSTH from an on-sustained unit from a control mouse is seen to have a longer latency when compared with an on-sustained unit from a VGB-treated mouse (B). (C) The FSLs from treated units (n = 495) showed a significant decrease of 4.0 ms, from 14.4 ms for control units (n = 492) to a mean FSL of 10.4 ms in treated units ($^{****}p < 0.0001$). Abbreviations: FSLs, first spike latencies; VGB, vigabatrin.

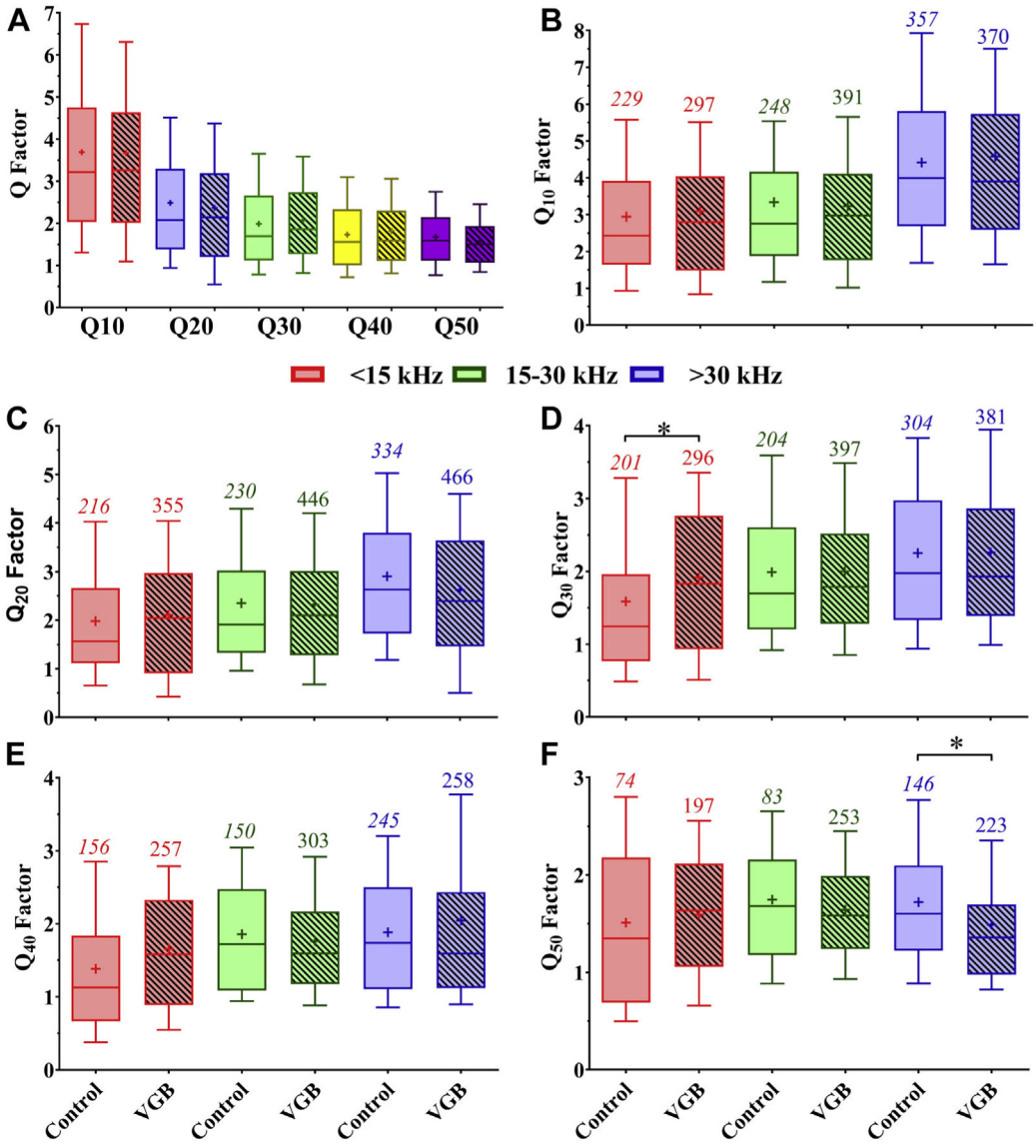

Fig. 8.

The filter bandwidth of the eFRAs calculated at 10, 20, 30, 40, and 50 dB above minimum threshold were not affected by VGB. (A) Overall Q-values combined for all frequency regions show a systematic decrease in Q with increases in intensity. These Q values were then divided by frequency region and showed minimal treatment effects, indicating that sharpness of observed eFRAs was not affected by VGB. Panels (B–F) show these frequency divided Q-values for levels above MT at 10 dB intervals. Significant differences were observed in only 2 regions of 2 different Q-values (*$p < 0.05$), the low-frequency units at Q30, shown in panel (D), and the high frequencies at Q50 values, shown in panel (F). Abbreviations: eFRA, excitatory frequency response areas; MT, minimum threshold; VGB, vigabatrin.

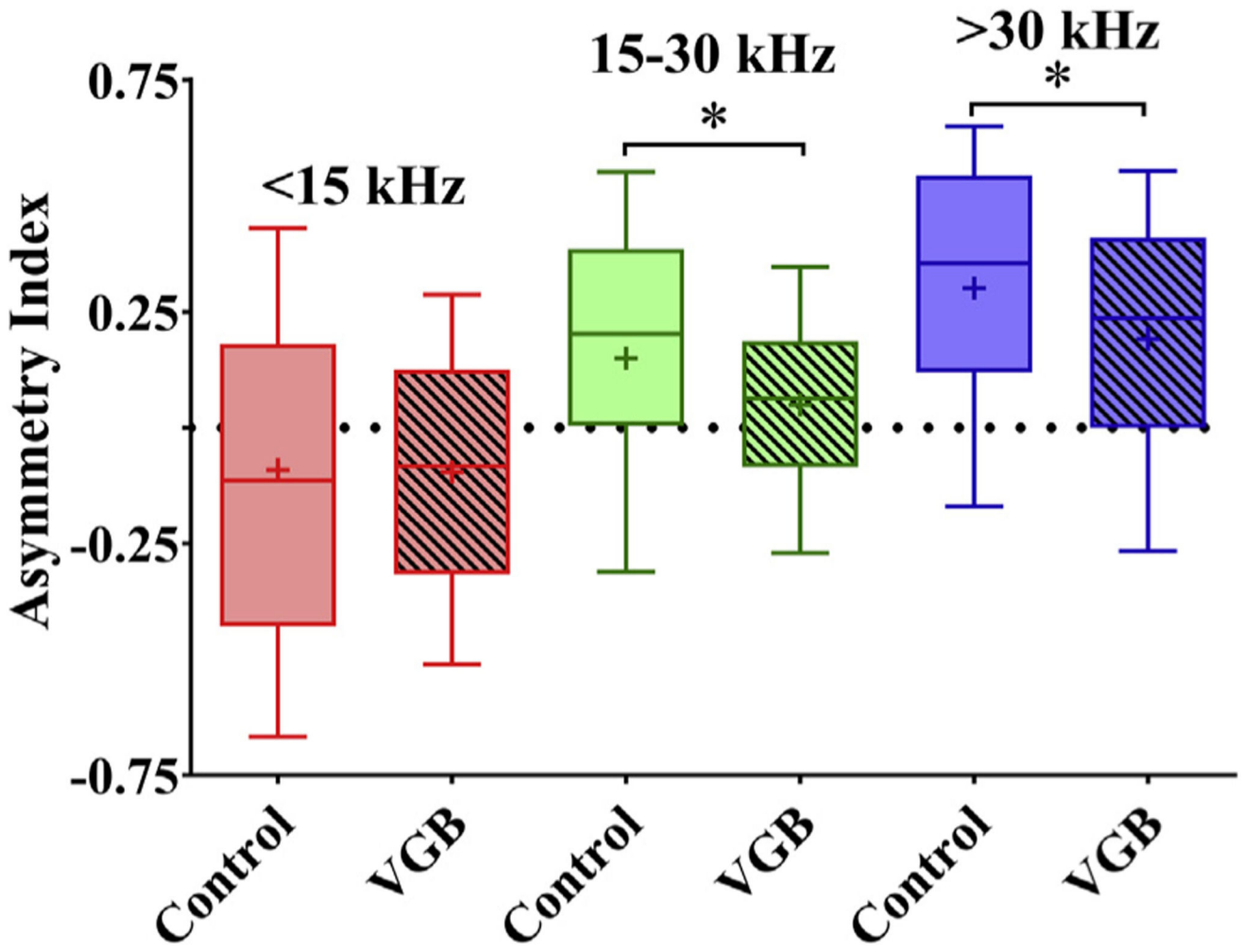

Fig. 9.

Asymmetry index of the excitatory receptive field is altered with VGB. The mean asymmetry index, measured from each eFRA, is plotted as a function of tonotopic region and shows that VGB-treated units were significantly different from controls. Calculated values range from −1 (tilted toward high frequencies) to +1 (tilted toward low frequencies), with 0 indicating a symmetrical eFRA. In general, the control units were significantly more asymmetrical than the other 2 groups across all tonotopic regions. Low-CF eFRAs in the treated mice trended toward being more symmetric, whereas the eFRAs of control animals were tilted toward high frequencies, with mean values of −0.090 and 0.095, respectively. The mid- and high-CF eFRAs of control animals were tilted more toward the low-frequencies (mean values 0.15 and 0.30) compared with the more symmetric receptive fields found in units from treated mice with observed mean values of 0.05 and 0.19 (*$p < 0.05$). Abbreviations: CFs, characteristic frequencies; eFRA, excitatory frequency response areas; VGB, vigabatrin.

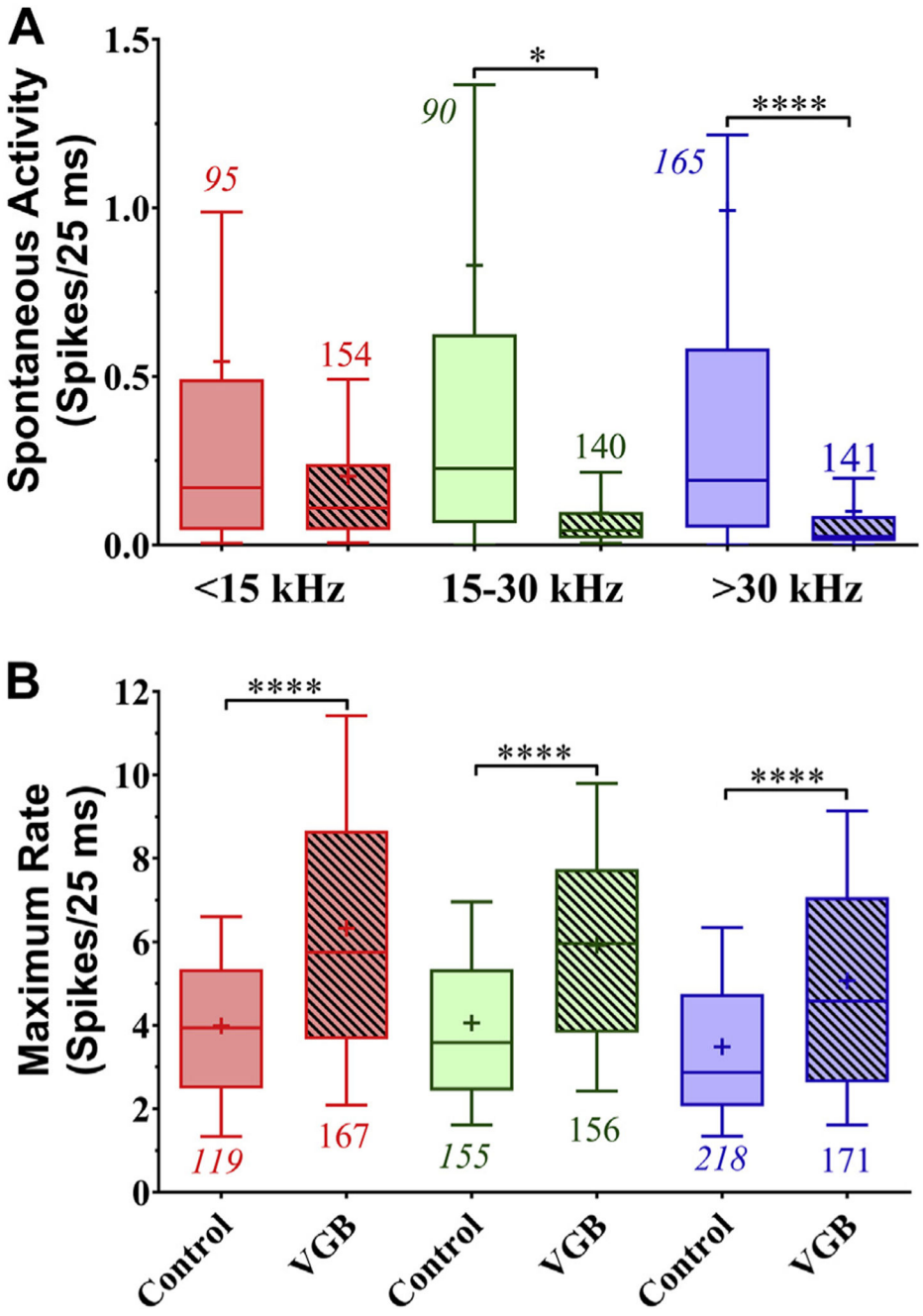

Fig. 10.

VGB treatment significantly decreased spontaneous activity while increasing driven rates. For the mid- and high-frequency tonotopic regions, spontaneous activity (A) was significantly decreased ($^{****}p < 0.0001$, $^{*}p < 0.05$) following VGB treatment. The maximum tone-evoked spike rates (B) showed significant increases for all frequencies following treatment ($^{****}p < 0.0001$). Abbreviation: VGB, vigabatrin.

Table 1

Distribution of the observed eFRA classification types

eFRA type	Total control units = 492					Total VGB-treated units = 495				
	V-type	U-type	Primary-like	Multi-peaked	Closed complex	V-type	U-type	Primary-like	Multi-peaked	Closed complex
Percent	72.7	15.6	5.2	4.5	1.9	52.5	23.9	16.9	2.8	3.8

Key: eFRA, excitatory frequency response areas; VGB, vigabatrin.